Journal of Medicinal Chemistry

pubs.acs.org/jmc Article

HDAC−Bax Multiple Ligands Enhance Bax-Dependent Apoptosis in HeLa Cells

Tao Liang, Yi Zhou, Reham M. Elhassan, Xuben Hou, Xinying Yang, and Hao Fang*

Cite This: https://dx.doi.org/10.1021/acs.jmedchem.0c01454 Read Online

ACCESS | Metrics & More | Article Recommendations | Supporting Information

ABSTRACT: Inspired by the synergistic effect of BTSA1 (a Bax activator) and SAHA (a histone deacetylase (HDAC) inhibitor) in HeLa cell growth suppression, a series of novel HDAC−Bax multiple ligands were designed rationally. Compound **23**, which possesses similar HDAC inhibitory activity relative to SAHA and Bax affinity comparable to BTSA1, exhibits a superior growth suppression against HeLa cells, and its antiproliferative activities are 15-fold and 3-fold higher than BTSA1 and SAHA, respectively. The better antiproliferative activity and lower cytotoxicity of compound **23** indicated that our HDAC−Bax multiple ligand design strategy achieved success. Further studies suggested that compound **23** could enhance Bax-dependent apoptosis by upregulating Bax, followed by inducing the conformational activation of Bax. To our knowledge, we first report HDAC−Bax multiple ligands and demonstrate a new paradigm for the treatment of solid tumors by enhancing Bax-dependent apoptosis.

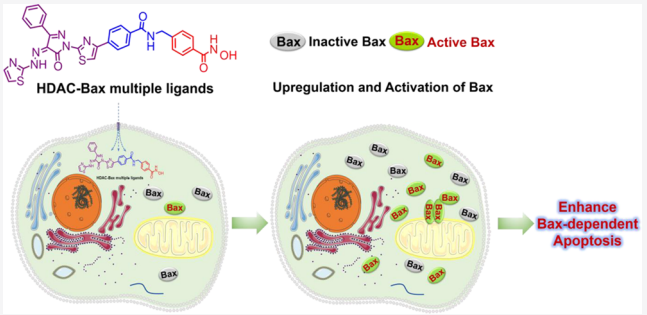

INTRODUCTION

As one of the most common gynecologic cancers, cervical cancer has a great effect on reproduction and even leads to causes of mortality in women.[1] The treatment of cervical cancer has changed dynamically over the past 20 years,[2] and more than two decades of efforts have promoted various effective therapeutic regimens, especially drug combination.[3−6] Accumulating evidence revealed that Bax is an essential key apoptotic mediator in cervical carcinoma cells, and activating Bax may be a new strategy for the treatment of cervical cancer.[7]

Bax, a key proapoptotic protein of the Bcl-2 family, is the cardinal regulator of the mitochondrial pathway.[8] Upon Bax conformational activation, oligomerization at the mitochondrial outer membrane (MOM) and mitochondrial outer membrane permeabilization (MOMP) occur, followed by the release of cytochrome *c*, Smac/DIABLO, and other apoptogenic factors, which turn on the caspase cascade of apoptosis[9−13] (Figure 1).

The activation of Bax could be achieved in an indirect manner (loss of antiapoptotic function) or a direct manner (gain of proapoptotic function).[14−17] For a long period of time, inhibiting the function of antiapoptotic proteins with Bcl-2, Mcl-1, or Bcl-X_L inhibitors is the most common indirect manner of Bax activation. However, identification of the first Bax activator BAM7 (half-maximal inhibitory concentration (IC_{50}) = 3.3 μM, Figure 2), which targets the Bax activation trigger site and induces conformational activation of Bax, provides blueprints for the development of alternative apoptosis regulators to induce Bax-dependent apoptosis directly.[18] Over 5 years of structural optimization efforts have led to the development of a series of potent Bax activators, such as Bax activator 8, BIF-44 as well as BTSA1[19−21] (Figure 2). BTSA1 (IC_{50} = 250 nM), the most potent Bax activator, exhibits good antiproliferative activity against human acute myeloid leukemia (AML) xenografts with acceptable toxicity.[19] Bax activators open up a new world for the accurate modulation of Bax-dependent apoptosis by flipping the "on switch" of Bax and demonstrate a new paradigm for pharmacologic induction of apoptosis.

Efforts of two decades have led to the development of five approved HDAC inhibitors (Vorinostat (SAHA), Romidepsin (FK228), Panobinostat (LBH-589), Belinostat (PXD101), and Chidamide (CS055), Figure 2) for the treatment of cutaneous T-cell lymphomas (CTCL), multiple myeloma (MM), and peripheral T-cell lymphomas (PTCL).[22−26] Accumulating evidence suggested that HDAC inhibition could upregulate Bax,[27−29] and we speculated that the combination of Bax activators and HDAC inhibitors may enhance Bax-dependent apoptosis and achieve better antiproliferation activities compared with single agents. To confirm our hypothesis, we combined BTSA1 and SAHA (1:1) in HeLa cells. Upon combination of both ligands, a better antiproliferative activity

Received: August 21, 2020

https://dx.doi.org/10.1021/acs.jmedchem.0c01454
J. Med. Chem. XXXX, XXX, XXX−XXX

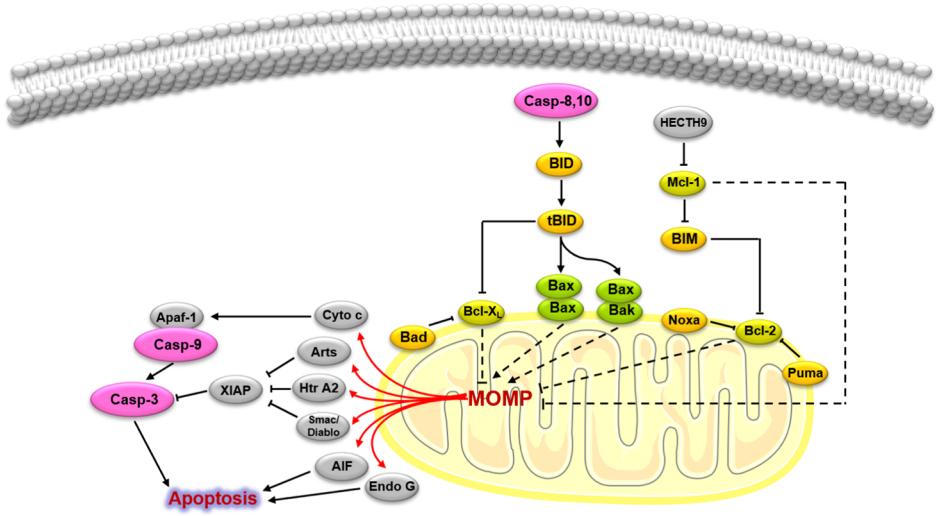

Figure 1. Apoptosis induced by Bax activation.

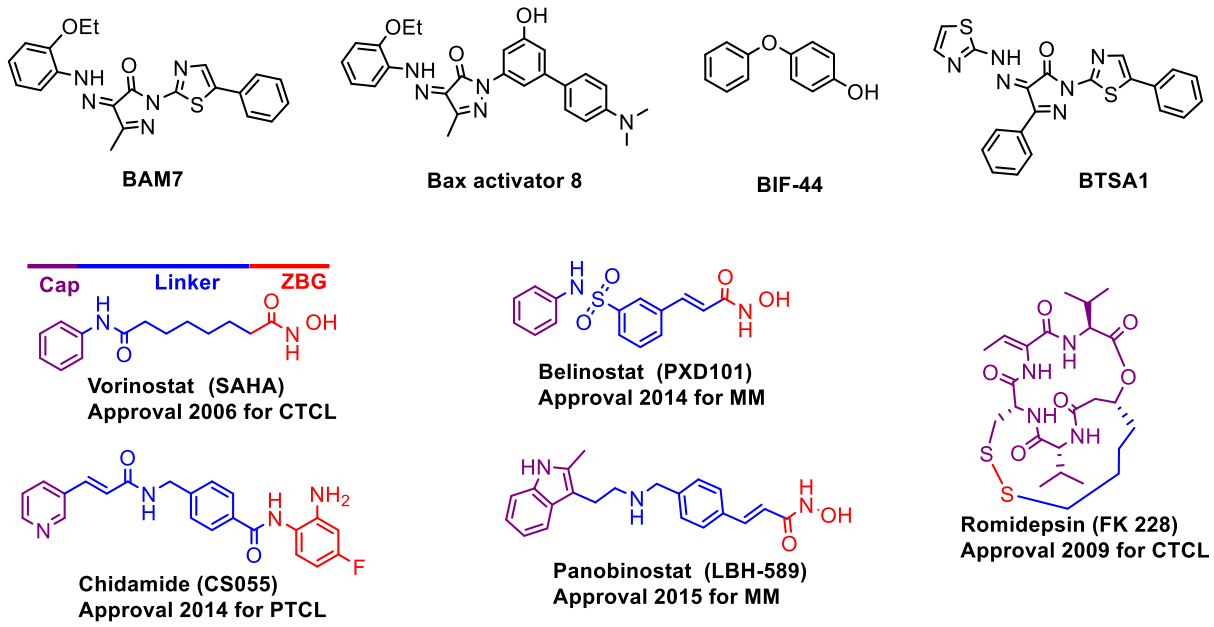

Figure 2. Bax activators and pharmacophores of representative histone deacetylase (HDAC) inhibitors.

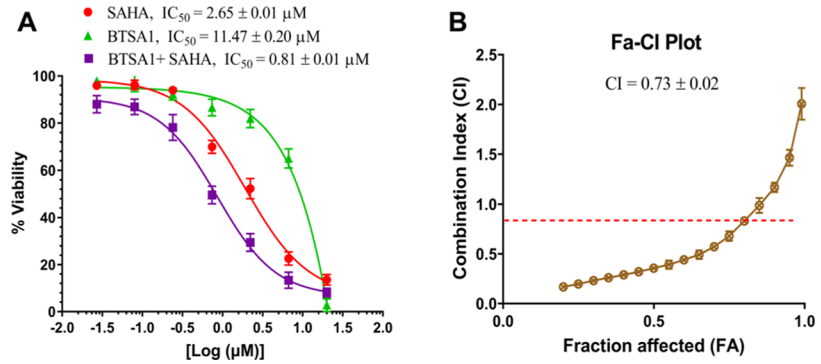

Figure 3. Combination (A) and the combination index (B) of BTSA1 and SAHA.

(IC_{50} = 0.81 μM) was observed in relation to monotherapy (BTSA1, IC_{50} = 11.47 μM; SAHA, IC_{50} = 2.65 μM, Figure 3A). We further analyzed the results using the Chou−Talalay method and calculated the combination index (CI) value with CompuSyn according to the dose−effect relationship. The combination index value of 0.73 indicated that the combination of SAHA and BTSA1 exhibits moderate synergistic effects in the growth suppression of HeLa cells

https://dx.doi.org/10.1021/acs.jmedchem.0c01454
J. Med. Chem. XXXX, XXX, XXX−XXX

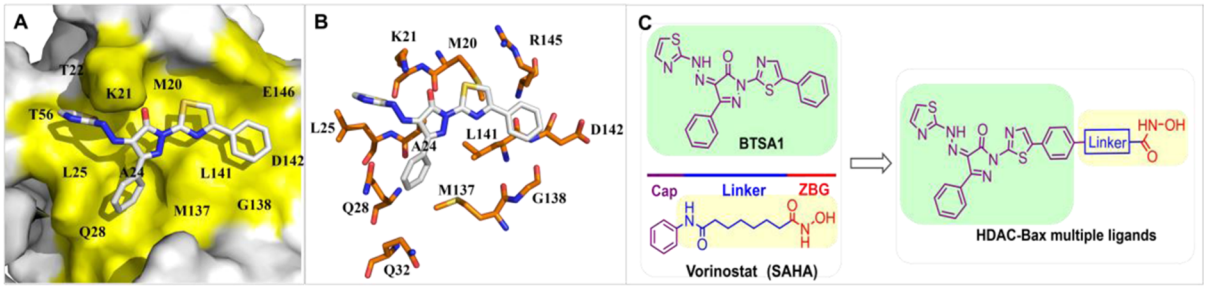

Figure 4. (A) Binding mode of BTSA1; (B) interactions between BTSA1 and Bax (PDB ID: 2K7W); (C) design of HDAC−Bax multiple ligands.

Scheme 1. Synthetic Route of Compounds 2−4[a]

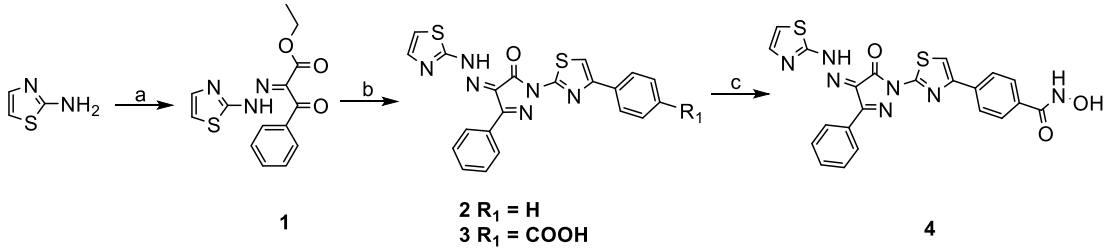

[a]Reagents and conditions: (a) (i) $NaNO_2$, HCl, H_2O, 0 °C, 30 min; (ii) CH_3COONa, ethyl benzoylacetate, EtOH, 0 °C, 1 h, 54%; (b) 2-bromoacetophenone or 4-(2-bromoacetyl)benzoic acid, thiosemicarbazide, EtOH, 80 °C, 47−48%; (c) isobutyl chlorocarbonate, *N*-methylmorpholine, THF, NH_2OH·HCl, KOH, MeOH, room temperature (rt), 6 h, 45%.

Scheme 2. Synthetic Route of Compounds 20−24[a]

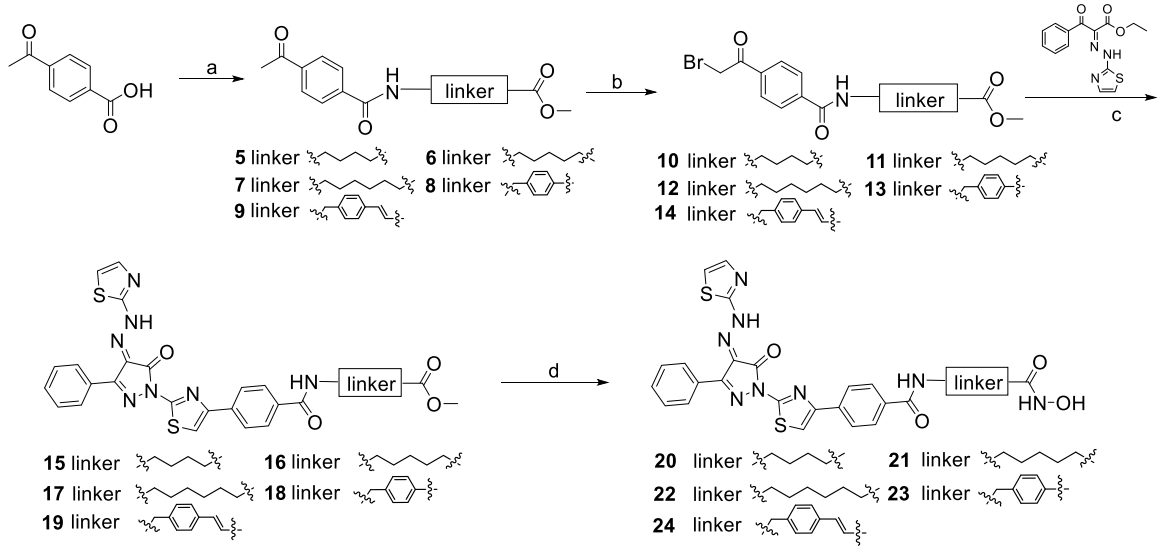

[a]Reagents and conditions: (a) HATU, DIPEA, CH_2Cl_2, rt, overnight, 67−99%; (b) $CuBr_2$, ethyl acetate/$CHCl_3$ (1:1), 80 °C, 3 h, 63−80%; (c) thiosemicarbazide, MeOH, 80 °C, 3 h, 33−68%; (d) NH_2OH·HCl, KOH, MeOH, rt, 6 h, 29−77%.

(Figure 3B). Encouraged by the moderate synergistic effect of the combination of BTSA1 and SAHA, we set out to explore more.

Drug combination is widely used in the treatment of a wide range of dreadful diseases, such as cancer and acquired immunodeficiency syndrome (AIDS), because of the synergistic therapeutic effect, dose and toxicity reduction, and to minimize or delay the induction of drug resistance.[30−33] Despite the benefit of drug combination, complex clinical trial design, complicated drug−drug interactions (DDIs), poor patient compliance, as well as unpredictable pharmacokinetics (PK) and pharmacodynamic (PD) relationship limit the application of drug combination.[34] However, multitarget drugs could solve these problems perfectly on the basis of retaining efficacy.[35−37] Therefore, we set out to develop HDAC−Bax multiple ligands, which could achieve HDAC inhibition and Bax conformational activation, for the treatment of cervical cancer.

Actually, it can be challenging to design multitarget agents because of the completely different structures of target proteins, and matching potencies at two separate targets with a single chemical entity is extremely difficult.[38] Our group designed and developed histone deacetylase and proteasome dual inhibitors using pharmacophore models.[39] To merge two

https://dx.doi.org/10.1021/acs.jmedchem.0c01454
J. Med. Chem. XXXX, XXX, XXX−XXX

Scheme 3. Synthetic Route of Compounds 46−52[a]

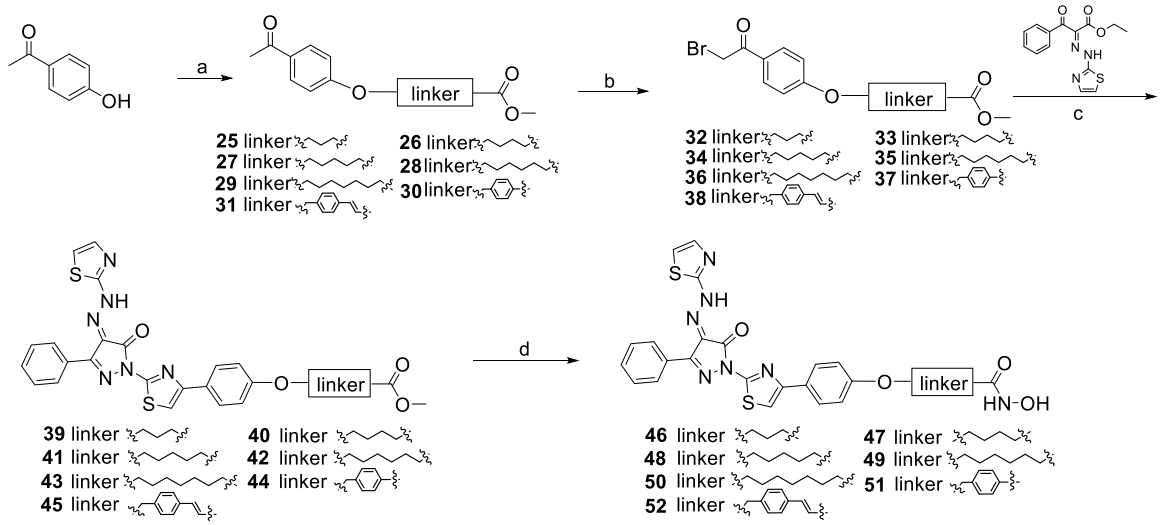

[a]Reagents and conditions: (a) K_2CO_3, rt, overnight, 83−94%; (b) $CuBr_2$, ethyl acetate/$CHCl_3$ (1:1), 80 °C, 3 h, 53−84%; (c) thiosemicarbazide, MeOH, 80 °C, 3 h, 52−78%; (d) $NH_2OH{\cdot}HCl$, KOH, MeOH, rt, 6 h, 55−83%.

different fragments (HDAC inhibitors and Bax activators), docking experiments (Figure 4A,B) and molecular dynamics (MD) simulation (Figure S71) were performed. BTSA1 was calculated to bind in the hydrophobic region at the juxtaposition of helices α1 and α6, and the thiazole group of BTSA1 lies adjacent to a presumed hinge site for loop opening upon initiation of the conformation activation of Bax. Moreover, the phenyl group attached to the pyrazolone core accommodates the Bax surface properly. This fragment is essential for Bax affinity, and replacement of the phenyl group with the methyl group resulted in decreased affinity.[19] Therefore, the pyrazolone core, the thiazole group, and the phenyl group attached to the pyrazolone are crucial for BTSA1 to achieve Bax affinity. HDAC inhibitors have a well-accepted pharmacophore: the zinc binding group (ZBG), the linker, as well as the cap group[40] (Figure 2), and these fragments are essential for HDAC inhibitory activity. Given the importance of the functional fragments (pyrazolone core, thiazole group, and phenyl group attached to the pyrazolone), we set up to use these functional fragments as the cap group and introduce a linker and ZBG at the solvent-exposed fragment, the 4-phenylthiazole group (Figure 4C).

To our knowledge, we first explored the combination of Bax activator and HDAC inhibitor and designed a series of novel HDAC−Bax multiple ligands rationally. Potent compound **23**, which possesses similar HDAC inhibitory activity relative to SAHA and Bax affinity comparable to BTSA1, exhibits better growth suppression against HeLa cells, and its antiproliferative activity is 15-fold and 3-fold better than BTSA1 and SAHA, respectively. Herein, we report the design, synthesis, and biological evaluation of our HDAC−Bax multiple ligands.

RESULTS AND DISCUSSION

Chemistry. The synthetic methods for target compounds are depicted in Scheme 1−3. Thiazol-2-amine was transformed into diazonium salt, which was used to synthesize ethyl (*Z*)-3-oxo-3-phenyl-2-(2-(thiazol-2-yl)hydrazono)propanoate (**1**) in the presence of ethyl benzoylacetate. Target compounds **2** and **3** were prepared starting from intermediate **1** and thiosemicarbazide in the presence of 2-bromoacetophenone or 4-(2-bromoacetyl)benzoic acid in boiling ethanol for 3 h. Moreover, target compound **4** was synthesized by converting the carboxyl group of target compound **3** into hydroxamic acid using isobutyl chlorocarbonate, *N*-methylmorpholine, and hydroxylamine hydrochloride in tetrahydrofuran (THF). For the second series of target compounds, 4-carboxybenzaldehyde was coupled with different amino acid derivatives for the synthesis of intermediates **5−9** by amide coupling reactions in the presence of 1-[bis(dimethylamino)methylene]-1*H*-1,2,3-triazolo[4,5-*b*]pyridinium 3-oxid hexafluorophosphate (HATU) and *N*,*N*-diisopropylethylamine (DIPEA) in CH_2Cl_2. Copper(II) bromide was simply used for the bromination reactions to prepare intermediates **10−14**, which were converted into key intermediates **15−19** in a manner similar to that described for the preparation of compound **2**. Finally, intermediates **15−19** were converted into target compounds **20−24** in the presence of hydroxylamine hydrochloride and potassium hydroxide in *N*,*N*-dimethylformamide (DMF) (Scheme 2). As for the third series of HDAC−Bax multiple ligands, different alkylation reactions of 4′-hydroxyacetophenone were performed to obtain intermediates **25−31** in the presence of K_2CO_3 and KI in DMF. Then, the syntheses of target compounds **32−52** were similar to that described for the preparation of the second series of target compounds **15−24** (Scheme 3).

Biological Results. *Fluorescence Polarization Binding Assay.* The binding affinities of target compounds for the recombinant Bax protein were measured *in vitro* by the fluorescence polarization assay (FPA) that target compounds displace a fluorescein-labeled stapled peptide of the BIM BH3 helix, FITC-BIM from the Bax trigger site.[16] As shown in Table 1, most target compounds demonstrated similar Bax affinities because of the same fragments of Bax activators. Moreover, the most potent compound **23**, which displaced FITC-BIM from the Bax trigger site with an EC_{50} value of 392.9 nM, exhibited Bax affinity comparable to that of BTSA1 (target compound **2**, EC_{50} = 278.1 nM). Docking studies (Figure S70) revealed that compound **23** and BTSA1 share a similar binding mode within the Bax rear site. Structure−activity relationship (SAR) analysis indicated that the linker and the ZBG group of our

https://dx.doi.org/10.1021/acs.jmedchem.0c01454
J. Med. Chem. XXXX, XXX, XXX−XXX

Table 1. HDAC Inhibitory Activities and Bax Affinities of Target Compounds[a]

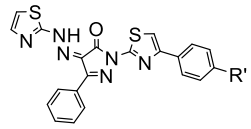

Compd	R′	EC_{50} (nM)[a] Bax	IC_{50} (nM)[a] HDACs
3		703.9 ± 3.7	>10000
4		873.9 ± 40.5	577.4 ± 18.4
20	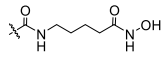	719.3 ± 60.3	207.4 ± 6.6
21	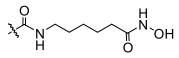	808.6 ± 34.0	87.5 ± 6.8
22	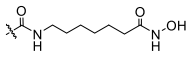	1143.9 ± 37.2	98.8 ± 7.1
23	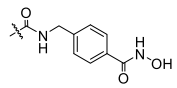	392.9 ± 18.1	62.8 ± 2.1
24	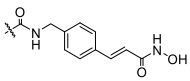	2218.1 ± 167.0	1341.5 ± 30.7
46	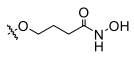	742.7 ± 89.3	674.8 ± 34.4
47	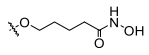	967.1 ± 114.1	118.5 ± 14.0
48	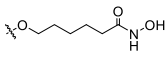	924.9 ± 59.1	75.8 ± 0.2
49	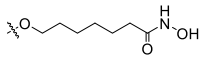	855.7 ± 18.9	40.8 ± 3.1
50	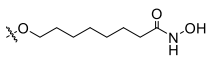	531.7 ± 56.8	135.2 ± 1.5
51	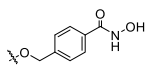	537.8 ± 4.8	85.0 ± 2.1
52	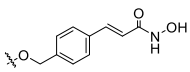	992.2 ± 531.3	243.7 ± 13.6
2 (BTSA1)	H	278.1 ± 41.0	> 10000
SAHA	–	> 10000	45.6 ± 1.2

[a]All compounds were assayed three times, and the results are expressed as mean ± standard error of the mean (SEM).

HDAC−Bax multiple ligands display different effects on Bax affinities. Short linkers exhibited slight effects on Bax affinities, whereas longer linkers or bulkier linkers impair the affinities for Bax, except for compound **50**. The longer and bulkier linkers of HDAC−Bax multiple ligands appear to affect the binding poses of the Bax activator fragments of target compounds within the Bax rear site.

In Vitro HeLa Cell Extract Inhibitory Assay. We next evaluated the HDAC inhibitory activities of all target compounds using the HeLa cell extract (containing primarily HDAC1 and HDAC2) with SAHA as the reference. The results in Table 1 suggest that some compounds exhibit good inhibitory activities against the HeLa cell extract. Target compound **2** (BTSA1, IC_{50} > 10 000 nM) without the ZBG

https://dx.doi.org/10.1021/acs.jmedchem.0c01454
J. Med. Chem. XXXX, XXX, XXX−XXX

Table 2. Selective Profiles of Compound 23 for Bcl-2 Family Proteins and the HDAC Isoform

	IC_{50} (nM)[a]					
	Bcl-2 family proteins			HDACs isoform		
	Bcl-2	Mcl-1	Bcl-X_L	HDAC1	HDAC2	HDAC8
23	>10 000	>10 000	>10 000	66.0 ± 2.3	197.9 ± 8.1	1086.8 ± 42.1
BTSA1	>10 000	>10 000	>10 000	ND[b]	ND	ND
SAHA	ND	ND	ND	39.8 ± 2.1	128.9 ± 4.5	2736.9± 151.0

[a]The results are expressed as mean ± SEM ($n \geq 2$). [b]ND, not detected.

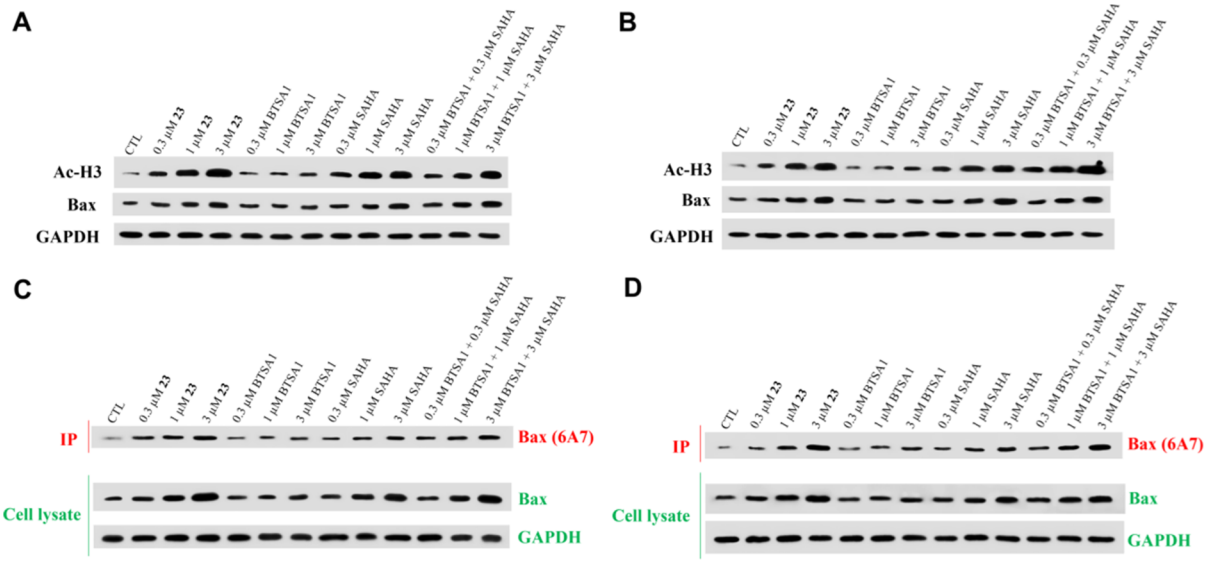

Figure 5. Upregulation and activation of the Bax in HeLa cells. Western blot analysis of samples incubated with compound **23**, BTSA1, SAHA, and BTSA1 + SAHA for 6 h (A) and 12 h (B); immunoprecipitation assay of samples incubated with compound **23**, BTSA1, SAHA, and BTSA1 + SAHA for 6 h (C) and 12 h (D).

group and target compound **3** (IC_{50} > 10 000 nM) with the carboxyl group as ZBG are inactive due to the poor chelation with the zinc ion of HDACs. Moreover, target compound **4** (IC_{50} = 557.3 nM) with hydroxamic acid as ZBG showed mild inhibitory activities against the HeLa cell extract because its linker is too short to accommodate the deep catalytic channel of HDACs (HDAC1 and HDAC2), and this prevents ZBG from chelating with the zinc ion well. Therefore, a suitable linker and ZBG are necessary pharmacophores for HDAC inhibitor activities. For the second series of HDAC−Bax multiple ligands, we explored the suitable linkers of target compounds. Compounds **21** and **23**, which possess suitable linkers, displayed good HDAC inhibitory activities (IC_{50} = 87.5 and 62.8 nM, respectively), whereas compound **20** (IC_{50} = 207.4 nM) with a shorter linker and compound **24** (IC_{50} = 1341.5 nM) with a longer linker showed weaker HDAC inhibition. As for the third series of target compounds, they share a similar structure−activity relationship (SAR) with the second series of compounds. Compounds **48**, **49**, and **51** could bury into the HDAC catalytic channel and chelate with zinc ions properly, which give them good HDAC inhibitory activities. In addition, potent target compound **23**, which exhibits good Bax affinity and HDAC inhibitory activity, was chosen for subsequent biological evaluation.

Selectivity Profile of Bcl-2 Family Proteins and HDACs. Bax activation can be achieved in an indirect manner (loss of antiapoptotic function with antiapoptotic protein inhibitors) or a direct manner (gain of proapoptotic function with Bax activators). To identify that our HDAC−Bax multiple ligands induce Bax activation directly instead of inhibiting the function of antiapoptotic proteins (Bcl-2, Mcl-1, and Bcl-X_L), the affinities of compound **23** for Bcl-2, Mcl-1, and Bcl-X_L were determined using the competitive fluorescence polarization binding Assay. Compound **23** showed no significant inhibition against Bcl-2, Mcl-1, and Bcl-X_L at the concentration of 10 μM (Table 2). In other words, compound **23** targets Bax specifically without binding to antiapoptotic proteins (Bcl-2, Mcl-1, and Bcl-X_L). On the other hand, we further explored HDAC isoform inhibitory profiles of compound **23**, and it showed good inhibitory activities against HDAC1 (IC_{50} = 66.0 nM) and HDAC2 (IC_{50} = 197.9 nM) and mild inhibition over HDAC8 (IC_{50} = 1086.8 nM). The result is consistent with the *in vitro* HeLa cell extract inhibitory assay.

Upregulation and Activation of Bax in HeLa Cells. Our HDAC−Bax multiple ligands contain two fragments of the HDAC inhibitor as well as a Bax activator, and they are supposed to upregulate and activate Bax. To confirm this, Western blot and immunoprecipitation assays were performed in HeLa cells. Following compound **23**, BTSA1, and SAHA treatment for 6 and 12 h, HeLa cells were harvested and lysed. Lysates were first analyzed to explore the expression of the Bax protein with the anti-Bax primary antibody (Cell Signaling cat. 2772) using Western blot. As shown in Figure 5A,B, compound **23** and the positive reference SAHA increase the acetylation of H3 (a major substrate of class I HDACs), indicating that they exhibit good HDAC inhibition. Moreover, compound **23** and SAHA could upregulate Bax compared with the control (CTL).

https://dx.doi.org/10.1021/acs.jmedchem.0c01454
J. Med. Chem. XXXX, XXX, XXX−XXX

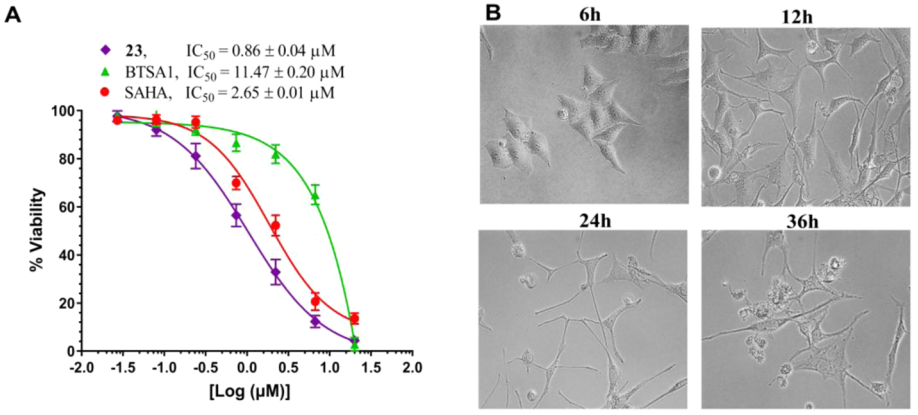

Figure 6. (A) Antiproliferative activities of compound **23**, BTSA1, and SAHA; (B) apoptotic morphologic features of HeLa cells in response to compound **23** (1 μM).

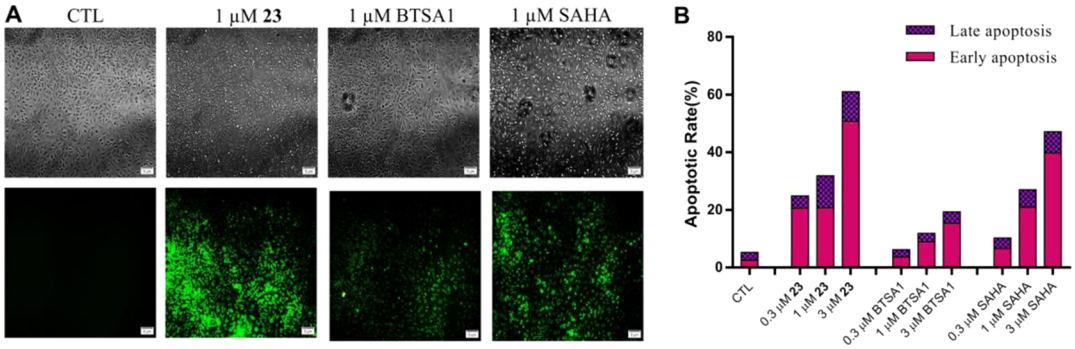

Figure 7. (A) TUNEL assay in HeLa cells treated with 1 μM compound **23**, BTSA1, and SAHA; (B) apoptosis induction of compound **23**, BTSA1, and SAHA in HeLa cells.

Subsequently, Bax conformational activation was determined with the conformation-specific primary antibody 6A7 (Santa Cruz, sc-23959), which recognizes the exposure of the Bax activation epitope. Lysates were immunoprecipitated with protein A agarose beads (Cell Signaling cat. 9863) and the anti-Bax antibody 6A7 overnight at 4 °C and then the beads were collected and analyzed using Western blot with the other anti-Bax primary antibody (Cell Signaling cat. 2772). Figure 5C,D suggests that compound **23** could induce the conformation activation of Bax more effectively in a dose-dependent manner compared with BTSA1. In addition, the ability of compound **23** to induce Bax conformation activation is comparable to that of BTSA1/Vorinostat cotreatment. These results indicated that compound **23** could achieve two proapoptotic functions in HeLa cells: (1) upregulate Bax and (2) induce the conformation activation of Bax.

Cell Viability and Morphologic Features. We evaluated the antiproliferative activity of compound **23** against HeLa cells. In the range of concentrations tested, compound **23** exhibits a better property concerning suppression of HeLa cell growth (IC_{50} = 0.86 μM) compared with BTSA1 (IC_{50} = 11.47 μM) and SAHA (IC_{50} = 2.67 μM) (Figure 6A), and its antiproliferative activities are 3 and 15 times better than those SAHA and BTSA1, respectively. Compound **23**, which possesses HDAC inhibitory activity and Bax affinity comparable to SAHA and BTSA1, respectively, exhibits better antiproliferative activity against HeLa cells, illuminating the fact that our HDAC−Bax multiple ligand design strategy achieves success.

Moreover, we monitored the morphology changes of HeLa cells in response to compound **23** (1 μM). Upon treatment of HeLa cells with compound **23**, a wide range of apoptotic morphologic features was observed, such as progressive cellular shrinkage, membrane blebbing, and the formation of apoptotic bodies (Figure 6B). Given the apoptotic morphologic features of HeLa cells, we speculated that our compound **23** suppresses the growth of HeLa cells by inducing apoptosis.

Terminal Deoxynucleotidyl Transferase (TdT) Deoxyuridine Triphosphate (dUTP) Nick-End Labeling (TUNEL) Assay and Flow Cytometry Analysis. The terminal deoxynucleotidyl transferase (TdT) dUTP nick-end labeling (TUNEL) assay was designed and performed to confirm whether compound **23** induces apoptosis in HeLa cells. The strong green fluorescence of HeLa cells (Figure 7A) treated with compound **23** (1 μM) indicated that compound **23** could induce apoptosis in HeLa cells effectively. To further determine the apoptotic rate of HeLa cells in response to compound **23**, flow cytometry analysis (annexin V/propidium iodide (PI) staining) was conducted. Compound **23** induces apoptosis of HeLa cells effectively at the indicated concentration, and over 60% of apoptotic HeLa cells were detected after incubating with 3 μM compound **23** for 48 h (Figure 7B). However, the positive controls SAHA and BTSA1 exhibit weaker apoptosis induction (apoptotic rates are 47.1 and 19.2%, respectively). In addition, compound **23** also induces apoptosis more effectively in HeLa cells at lower concentrations (0.3 and 1 μM) compared to the positive controls.

Mitochondrial Depolarization Assay (mtΔΨ) and Caspase-3 Activation Assay. Bax conformational activation,

https://dx.doi.org/10.1021/acs.jmedchem.0c01454
J. Med. Chem. XXXX, XXX, XXX−XXX

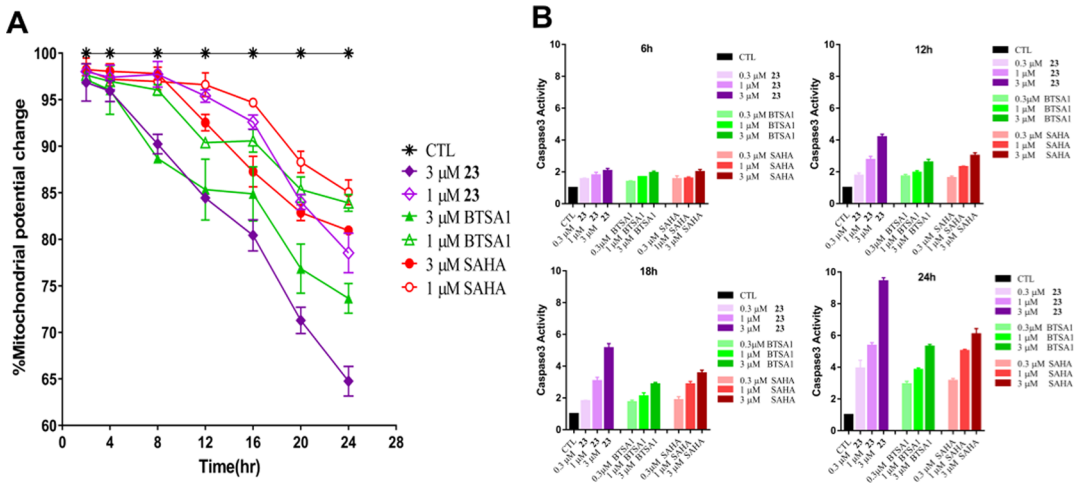

Figure 8. (A) TMRE mitochondrial potential assay in HeLa cells treated with serial dilution doses of compound **23**, BTSA1, and SAHA at indicated time points; (B) caspase-3 activity in HeLa cells incubated with indicated concentrations of compound **23**, BTSA1, and SAHA.

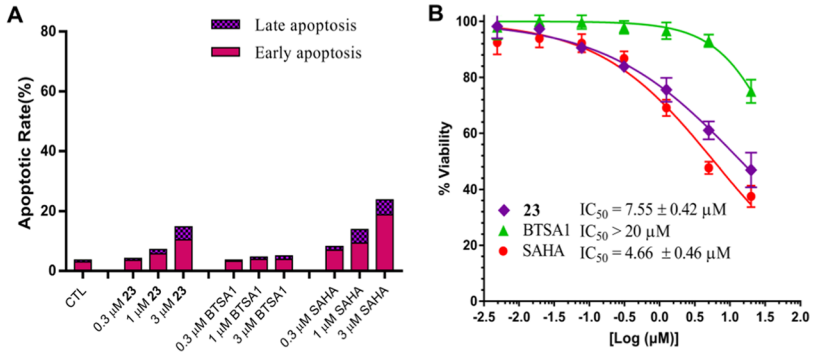

Figure 9. (A) Apoptosis induction in HeLa cells Bax$^{-/-}$ of compound **23**, BTSA1, and SAHA; (B) viability assay of HeLa cells Bax$^{-/-}$ treated with compound **23**, BTSA1, and SAHA for 48 h.

translocation, and oligomerization at the mitochondrial outer membrane (MOM) result in mitochondrial outer membrane permeabilization (MOMP), followed by the release of cytochrome *c*, Smac/Diablo, and other mitochondrial factors, thereby initiating the caspase cascade of apoptosis.[33] Therefore, we monitored mitochondrial potential changes and caspase-3 activation of HeLa cells in response to compound **23**, BTSA1, and SAHA. Upon compound **23**, BTSA1, and SAHA treatment, the mitochondrial potential changes were determined with tetramethylrhodamine ethyl ester (TMRE, Sigma cat. 87917). Mitochondrial potential loss was detected in HeLa cells incubated with compound **23**, BTSA1, and SAHA, but our compound **23** could induce mitochondrial depolarization more effectively in a dose-responsive manner and a time-dependent manner (Figure 8A).

In addition, caspase-3 activation in response to compound **23** was determined with the caspase-3 fluorometric assay kit (Biovision, K105-200) in HeLa cells. The results (Figure 8B) revealed that upon treatment of HeLa cells with compound **23** for different times (6, 12, 18, and 24 h), the amount of activated caspase-3 is significantly increased compared with the control (CTL). All tested compounds induced the activation of caspase-3 in a dose-dependent manner and a time-dependent manner, and compound **23** exhibits the best property concerning caspase-3 activation.

Bax Knockdown in HeLa Cells. To prove that compound **23** can induce Bax-dependent apoptosis in HeLa cells, the Bax protein was knocked down using siRNA (RIBOBIO, cat. stB0003578A). Subsequently, the apoptotic rates of HeLa cells Bax$^{-/-}$ in response to compound **23**, BTSA1, and SAHA were determined using flow cytometry analysis (annexin V/PI staining). Figure 9A suggests that Bax knockdown greatly impaired the ability of compound **23** to induce apoptosis in HeLa cells Bax$^{-/-}$ (14.8% apoptotic rate at 3 μM) and even abolished the ability of BTSA1 to induce apoptosis, whereas Bax knockdown shows less impact on SAHA.

We further evaluated the antiproliferative activities of compound **23**, BTSA1, and SAHA against HeLa cells Bax$^{-/-}$. Compound **23** and BTSA1 exhibited weaker antiproliferative activities against HeLa cells Bax$^{-/-}$ (Figure 9B, compound **23**, IC_{50} = 7.55 μM; BTSA1, IC_{50} > 20 μM) compared with wild-type HeLa cells (compound **23**, IC_{50} = 0.86 μM; BTSA1, IC_{50} = 11.47 μM). Bax knockdown greatly impaired the antiproliferative activity of compound **23** and even abolished the antiproliferative activity of BTSA1. However, the antiproliferative activity of SAHA against HeLa cells Bax$^{-/-}$ (IC_{50} = 4.66 μM) is comparable to that of wild-type HeLa cells (IC_{50} = 2.65 μM).

These results indicated that compound **23** and BTSA1 suppress the growth of HeLa cells by inducing Bax-dependent apoptosis. However, Bax knockdown, which abolishes Bax-dependent apoptosis, greatly impaired the apoptosis induction of compound **23** and BTSA1 in HeLa cells Bax$^{-/-}$, followed by weaker antiproliferative activities.

https://dx.doi.org/10.1021/acs.jmedchem.0c01454
J. Med. Chem. XXXX, XXX, XXX−XXX

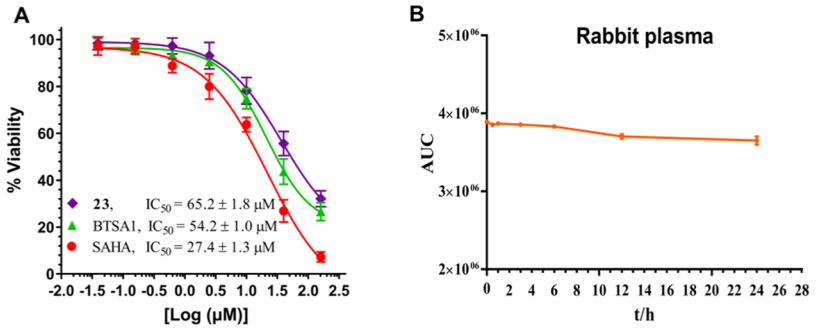

Figure 10. (A) Cytotoxicity of compound **23**, BTSA1, and SAHA on normal HL-7702 cells; (B) stability of compound **23** in rat plasma.

In Vitro Cytotoxicity Studies. Toxicity study is an inevitable issue in drug development, and the cytotoxicities of compound **23**, BTSA1, and SAHA were evaluated using healthy HL-7702 cells (human normal liver cells). All tested compounds exhibited acceptable cytotoxicity (Figure 10A), whereas BTSA1 (IC_{50} = 54.2 μM) and compound **23** (IC_{50} = 65.2 μM) exhibited lower cytotoxicity compared with SAHA (IC_{50} = 27.4 μM). Given the good antiproliferative activity against HeLa cells and acceptable cytotoxicity over normal HL-7702 cells, we conclude that compound **23** kills HeLa cells effectively and spares healthy cells.

*Stability of Compound **23** in Rabbit Plasma.* A preliminary investigation of the stability of compound **23** was performed. After incubating compound **23** with rabbit plasma at 37 °C for indicated times (0, 0.5, 1, 3, 6, 12, and 24 h), samples were analyzed using high-performance liquid chromatography (HPLC). The result (Figure 10B) shows that compound **23** is stable in rabbit plasma.

CONCLUSIONS

Encouraged by the better antiproliferative activity of the combination of BTSA1 and SAHA compared with a single drug, a series of novel HDAC−Bax multiple ligands were designed rationally. Preliminary evaluation revealed that all of the target compounds exhibit good profiles in a preliminary screening concerning HDAC inhibitory activities, Bax affinities, and Bax selectivity. Compound **23** possesses similar HDAC inhibitory activity relative to SAHA and Bax affinity comparable to BTSA1, whereas its antiproliferative activities are 15- and 3-fold better than BTSA1 and SAHA, respectively. The good antiproliferative activity and acceptable cytotoxicity of compound **23** indicated that the design strategy of HDAC−Bax multiple ligands is successful in HeLa cell growth suppression. In other words, the two fragments (HDAC inhibitor and Bax activator) of compound **23** achieve synergistic effects in suppression of HeLa cell growth. Moreover, a series of experiments confirmed that our compound **23** could upregulate Bax and induce the conformation activation of Bax, followed by initiating the intrinsic apoptosis pathway, thereby enhancing Bax-dependent apoptosis. In addition, the ability of compound **23** to induce Bax conformation activation is comparable to that of BTSA1/Vorinostat cotreatment. In summary, we first report the design, synthesis, and biological evaluations of HDAC−Bax multiple ligands, and our studies display a new paradigm for the treatment of solid tumor by enhancing Bax-dependent apoptosis.

EXPERIMENTAL SECTION

Biology. *Reagents.* Primary antibodies were purchased from Cell Signaling Technology (CST), Santa Cruz, Abcam, and Beyotime Biotechnology. HeLa cells (ATCC, CCL-2) were purchased from the American-type culture collection (ATCC). Salt, organic solvents, and other reagents were from Sigma-Aldrich, Cell Signaling Technology (CST), Biovision, Beyotime Biotechnology, and Ribobio Technology.

Production of Recombinant Protein. Human, recombinant Bax was expressed in transformed *Escherichia coli* BL21 (DE3), and protein expression was induced with 0.5 mM isopropyl β-D-1-thiogalactopyranoside (IPTG) in kanamycin-containing Luria Broth. For specific methods and more details, please refer to the Supporting Information.

Calculation of the Combination Index. The combination of BTSA1 and SAHA was performed, and the results were analyzed using the Chou−Talalay method.[30] The combination index (CI) value was calculated with CompuSyn according to the dose-inhibition relationship of the combination of SAHA and BTSA1 (1:1) or single drugs. Final CI results were the average of detailed CI values at inhibition rates of 0.5, 0.75, and 0.9 and expressed as mean ± SEM. Moreover, synergism is subdivided into (near) additive (CI = 1.0), slight synergism (CI value is within 0.85−1.0), moderate synergism (CI value is within 0.7−0.85), synergism (CI value is within 0.3−0.7), strong synergism (CI value is within 0.1−0.3), and very strong synergism (CI < 0.1).

Fluorescence Polarization Binding Assay. Bax Binding Assay. Direct binding curves were generated by incubating FITC-BIM (50 nM) with indicated dilutions of full-length His-Bax, and fluorescence polarization was measured at 30 min on an Envision station (PerkinElmer) under the condition of an excitation wavelength (480 nm) and an emission wavelength (535 nm). For competition assays, a serial dilution of test compounds or acetylated BIM (Ac-BIM) was incubated with full-length His-Bax (500 nM) for 30 min, followed by the addition of FITC-BIM (50 nM). After 20 min of incubation, fluorescence polarization was measured on an Envision station (PerkinElmer). EC_{50} or IC_{50} values were calculated by nonlinear regression analysis of dose−response curves with Graphpad Prism software.

Bcl-2, Mcl-1, and Bcl-X_L Binding Assays. 5-FAM Bid-BH3 direct binding curves to His-Bcl-2, His-Mcl-1, and His-Bcl-X_L were generated by incubating the fluorescent peptide (50 nM) with the indicated dilution of full-length recombinant purified proteins, and fluorescence polarization was measured at 30 min on an Envision station (PerkinElmer) under the condition of an excitation wavelength (485 nm) and an emission wavelength (535 nm). As for competition assays, a serial dilution of the tested compounds or ABT-199 was incubated with full-length His-Bcl-2 (500 nM), His-Mcl-1 (250 nM), or His-Bcl-X_L (200 nM) for 30 min, and 5-FAM Bid-BH3 (10 nM) was added. After 20 min, fluorescence polarization was measured on an Envision station (PerkinElmer). EC_{50} or IC_{50} values were calculated by nonlinear regression analysis of dose−response curves with GraphPad Prism software.

HDAC Inhibitory Assay. A fluorescence assay was used to evaluate HDAC inhibitory activities of target compounds, with SAHA as the

https://dx.doi.org/10.1021/acs.jmedchem.0c01454
J. Med. Chem. XXXX, XXX, XXX−XXX

reference. Briefly, an enzyme solution (HeLa nuclear extract, HDAC1, HDAC2, and HDAC8) was treated with a serial dilution of the tested compounds, followed by 5 min of incubation at 37 °C, and then the fluorogenic substrate Boc-Lys (acetyl)-AMC or Boc-Lys (trifluoroacetyl)-AMC was added. After 30 min of incubation at 37 °C, the reaction was quenched by the addition of a developer containing trypsin and trichostatin A (TSA). The suspension was incubated at 37 °C for 20 min, and the fluorescence intensity was monitored using a microplate reader at the excitation and emission wavelengths of 390 and 460 nm. The fluorescence intensity readings of the tested wells relative to those of the control wells were used to calculate the inhibition ratios and the IC_{50} values.

Western Blot. After treating with compound **23**, BTSA1, SAHA, or vehicle (0.2% dimethyl sulfoxide (DMSO)) for 6 and 12 h, HeLa cells were harvested and lysed with a radioimmunoprecipitation assay (RIPA) buffer containing 1 mM phenylmethylsulfonyl fluoride (PMSF) as well as 1% phosphatase inhibitor cocktail solution on ice for 30 min. Lysates were centrifugated at 4 °C, 14 000 rpm, and the supernatants were collected and boiled in loading buffer. Protein samples were electrophoretically separated on 12.5% sodium dodecyl sulfate (SDS) polyacrylamide gel electrophoresis (PAGE) gel (EpiZyme, PAGE gel fast preparation kit), transferred to immobilon-FL poly(vinylidene fluoride) (PVDF) membranes (Millipore), and subjected to immunoblotting. For visualization of proteins, membranes were blocked in TBST containing 5% nonfat dry milk. After washing three times with TBST, the membranes were incubated with primary antibodies overnight at 4 °C in a 1:1000 dilution. Then, membranes were washed with TBST and incubated with a secondary antibody in a 1:2000 dilution. Finally, the ECL reaction was performed using the Boster ECL kit, and membranes were detected on Amersham Imager 680. Proteins were detected following primary antibodies: Bax (Cell Signaling cat. 2772), Ac-H3 (Cell Signaling cat. 13998), and glyceraldehyde-3-phosphate dehydrogenase (GAPDH) (Beyotime, AF1186).

Immunoprecipitation Assay. Incubated with compound **23**, BTSA1, SAHA, or vehicle (0.2% DMSO) for 6 and 12 h, HeLa cells were harvested and lysed with NP-40 buffer containing 1 mM PMSF and 1% phosphatase inhibitor cocktail solution on ice for 30 min. Lysates were immunoprecipitated with protein A agarose beads (Cell Signaling cat. 9863) and the conformation-specific primary antibody 6A7 (Santa Cruz, sc-23959) that recognizes the exposure of the Bax activation epitope overnight at 4 °C. The beads were collected by centrifugation and then washed three times with NP-40 buffer, followed by boiling in a loading buffer. Protein samples were analyzed using Western blot in the presence of the anti-Bax primary antibody (Cell Signaling cat. 2772) and GAPDH (Beyotime, AF1186).

Cell Viability and Cytotoxicity Studies. HeLa cells and HeLa cells $Bax^{-/-}$ were cultured with the Roswell Park Memorial Institute (RPMI) 1640 medium (10% fetal bovine serum (FBS)) at 37 °C in a 5% CO_2 humidified incubator. In brief, the cells were seeded at 3500−4000 cells per well (100 μL/well) in 96-well plates for 8 h, followed by incubating with the indicated dilution of the tested compound (100 μL/well) for 48 h. The solution of 0.5% 3-(4,5-dimethyl-2-thiazolyl)-2,5-diphenyl-2-*H*-tetrazolium bromide (10 μL/well) was added, and the mixture was incubated for another 4 h. A total of 150 μL of DMSO was added and shaken for dissolution for 15 min at 37 °C. Absorbance was determined with a microtiter-plate reader at 570 nm to calculate the inhibition ratios and the IC_{50} values.

Moreover, cytotoxicity studies of compound **23**, TBSA1, and SAHA were evaluated in healthy HL-7702 cells (human normal liver cells) in a manner that was described for cell viability assays.

Cell Morphologic Features. HeLa cells were seeded at 1×10^5 cells per well (2 mL/well) in six-well clear-bottom plates. After 8 h of incubation at 37 °C in a 5% CO_2 humidified incubator, the solution of compound **23** (1 μM) was added, followed by incubating for 6, 12, 24, and 36 h. Then, cell morphology changes were monitored using a Zeiss Axio Observer A1 fluorescence microscope.

TUNEL Assay. Terminal deoxynucleotidyl transferase (TdT) dUTP nick-end labeling (TUNEL) assay was designed to detect apoptotic HeLa cells. HeLa cells (1×10^5) were incubated with 1 μM compound **23**, BTSA1, SAHA, or vehicle (0.2% DMSO) in six-well clear-bottom plates for 48 h and then washed with prechilled phosphate-buffered saline (PBS) two times. Then, these cells were fixed with paraformaldehyde for 30 min at rt. After treating PBS containing 0.5% Triton X-100 for 5 min, cells were washed with PBS three times, followed by the addition of a mixture of terminal deoxynucleotidyl transferase and FITC-12-dUTP. Finally, cells were washed two times carefully and green fluorescence was observed using laser confocal microscopy.

Flow Cytometry Analysis. Flow cytometry analysis was performed in HeLa cells and HeLa cells $Bax^{-/-}$. Cells (1×10^5 cells/well) were incubated with different concentrations (0.3, 1, and 3 μM) of compound **23**, BTSA1, SAHA, or vehicle (0.2% DMSO) in six-well clear-bottom plates for 48 h. Subsequently, cells were harvested by centrifugation and washed with cold PBS buffer. Cells were resuspended in 195 μL of annexin V−fluorescein isothiocyanate (FITC) binding buffer, and 2.5 μL of annexin V−FITC and 5 μL of propidium iodide (PI) were added. The samples were incubated for 15 min at room temperature and analyzed using flow cytometry.

Mitochondrial Depolarization Assay (mtΔΨ). Cells (1×10^5 cells/well) were seeded in six-well clear-bottom plates and incubated with the indicated dilution of compound **23**, BTSA1, SAHA, or vehicle (0.2% DMSO). Cells were stained with 100 nM tetramethylrhodamine ethyl ester (TMRE, Sigma cat. 87917) for 30 min at 37 °C. Subsequently, cells were collected by centrifugation and washed with PBS to eliminate background fluorescence. They were transferred into a black 96-well plate, and the fluorescence intensity was detected by a Thermo Varioskan microplate reader (Ex: 540 nm; Em: 579 nm).

Caspase-3 Activation Assay. HeLa cells were incubated with various concentrations (0.3, 1, and 3 μM) of potent compound **23**, BTSA1, SAHA, or vehicle (0.2% DMSO) for different times (6, 12, 18, and 24 h); then, 1×10^6 cells were collected and washed with PBS. Cells were resuspended with 50 μL of chilled cell lysis buffer on ice for 10 min, and the lyases were transferred into a 96-well plate. Then, 50 μL of 2× reaction buffer (containing 10 mM dithiothreitol (DTT)) and 5 μL of caspase-3 substrates (1 mM DEVE-AFC) were added to each sample, and the mixture was incubated at 37 °C for 1.5 h. The fluorescence intensity was tested in a microplate reader at the excitation and emission wavelengths of 400 and 505 nm. The results are expressed as fold increase in the caspase activity of apoptotic cells over that of noninduced cells.

Cellular Transfections. HeLa cells were transfected with siRNA of Bax to silence the Bax protein with the riboFECT CP transfection kit (RIBOBIO, Cat. C10511-05) according to the manufacturer's protocol. Generally, HeLa cells were incubated with a mixture of 1× riboFECT CP buffer, 50 nM siRNA of Bax as well as the riboFECT CP reagent and cultured with an RPMI 1640 medium (10% FBS) at 37 °C in a 5% CO_2 humidified incubator. After 24 and 72 h, cells were harvested and lysed with a RIPA buffer containing 1 mM PMSF and a 1% phosphatase inhibitor cocktail solution. Lysates were used to monitor the transfection efficiency with Western blot.

*Stability of Compound **23** in Rat Plasma.* First, 50 μL of compound solution (2 mg/mL in DMSO) and 200 μL of rabbit plasma were incubated at 37 °C for indicated times (0, 0.5, 1, 3, 6, 12, and 24 h). Then, 600 μL of acetonitrile was added into each sample aliquot, followed by centrifugation (14 000 rpm, 10 min) and filtration. Samples were analyzed using HPLC with a C_{18} column (150 mm × 4.6 mm, 5 μm, Diamonsil) at a flow rate of 1 mL/min. The mixture of 85% methanol and 15% H_2O containing 0.1% formic acid was used as the mobile phase.

Molecular Docking and Molecular Dynamics Simulation. The NMR structure of Bax (PDB ID: 2K7W) was selected for molecular docking experiments using GLIDE (Glide, version 11.5, Schrodinger). After protein preparation and grid generation, BTSA1 was docked into the Bax trigger site and top-scoring binding poses were chosen as the proposed binding modes. Then, the lowest-energy structure pose from docking was subjected to molecular dynamics (MD) simulation using DESMOND (DESMOND, version 3, Schrodinger); please refer

https://dx.doi.org/10.1021/acs.jmedchem.0c01454
J. Med. Chem. XXXX, XXX, XXX−XXX

to a previous report.[19] Clustering and analysis of the trajectory were performed with MAESTRO tools (Maestro, version 10.0, Schrodinger).

Moreover, compound **23** was docked into Bax in a manner similar to those described for the docking studies of BTSA1, and the results are displayed in the Supporting Information.

Chemistry. In our work, all start materials, reagents, and solvents are analytical grade and used without further purification unless otherwise stated. Reactions were monitored by thin-layer chromatography (TLC) on 0.25 mm silica gel plates (60GF-254), and the spots were visualized with UV light, chloride ferric, and iodine vapor. Melting points were determined by the RY-1 electrothermal melting point apparatus. ^{1}H NMR and ^{13}C NMR spectra were obtained on a Brucker DRX spectrometer at 400 MHz. Chemical shifts are shown in parts per million (ppm) relative to tetramethylsilane (TMS) as the internal standard and are significant. ^{1}H NMR data are reported in the following order: multiplicity (m, multiplet; q, quartet; t, triplet; d, doublet; s, singlet) number of protons. High-resolution mass spectra (HRMS) were conducted on an Agilent 6510 quadrupole time-of-flight liquid chromatography/mass spectrometer (LC/MS) delivered with electrospray ionization (ESI). The purities of all of the target compounds were determined by reversed-phase (RP)-HPLC with a Shimadzu LC-20AT system and a C_{18}-silica column (Thermo, 4.6 × 150 mm^2, 5 μm). Elution was methanol/water (80:20−90:10), and the flow rate was 1 mL/min. All of the final compounds achieved a minimum of 95% purity.

*Ethyl (Z)-3-Oxo-3-phenyl-2-(2-(thiazol-2-yl)hydrazono)-propanoate (**1**).* To a solution of 2-aminothiazole (8 g, 80 mmol) in 6 M HCl (112 mL) at 0 °C, a solution of sodium nitrite (6.62 g, 96 mmol) in water (64 mL) was added dropwise while the temperature of the reaction mixture was maintained below 5 °C. When the addition was completed, the resulting diazonium salt was stirred for 30 min at 0 °C. A solution of sodium acetate (38 g, 460.8 mmol) in water (80 mL) was added to a solution of active ethyl benzoylacetate (12.30 g, 64 mmol) in ethanol (240 mL). The mixture was cooled to 0 °C, and the diazonium salt solution was added over a period of several mines. Then, the mixture was stirred for 1 h at 0 °C and for another 1 h at room temperature. Ethanol was reduced in vacuo and then extracted with ethyl acetate (200 mL × 3). The organic phase was combined and dried with anhydrous magnesium sulfate. Then, the organic phase was concentrated in vacuo to give the crude product, followed by purification using silica gel column chromatography with petroleum ether/ethyl acetate to obtain an orange-red oil 10.5 g, yield: 54%. ^{1}H NMR (400 MHz, $CDCl_3$) δ 12.80 (s, 1H), 7.96 (d, J = 7.7 Hz, 2H), 7.61 (t, J = 7.4 Hz, 2H), 7.48 (t, J = 7.7 Hz, 2H), 7.39 (d, J = 3.6 Hz, 1H), 6.84 (d, J = 3.5 Hz, 1H), 4.37 (q, J = 7.2 Hz, 2H), 1.32 (t, J = 7.1 Hz, 3H).

*(Z)-5-Phenyl-2-(4-phenylthiazol-2-yl)-4-(2-(thiazol-2-yl)-hydrazono)-2,4-dihydro-3H-pyrazol-3-one (**2**).* To a solution of 2-bromoacetophenone (0.33 g, 1.66 mmol) in ethanol (20 mL), thiosemicarbazide (0.15 g, 1.66 mmol) was added, and the mixture was stirred for 1 h at room temperature. When the addition of the solution of intermediate **1** (0.5 g, 1.66 mmol) in ethanol was completed, it was refluxed for 3 h. The reaction mixture was cooled down, and the product was isolated by filtration. It was washed with cool ethanol as well as diethyl ether, and the title compound was obtained as a red solid 0.4 g, yield: 47%, mp 230−231 °C. ^{1}H NMR (400 MHz, DMSO-d_6) δ 8.17 (d, J = 7.2 Hz, 2H), 8.01 (d, J = 7.6 Hz, 2H), 7.85 (s, 1H), 7.73 (d, J = 4.1 Hz, 1H), 7.61−7.53 (m, 3H), 7.48 (t, J = 7.6 Hz, 2H), 7.42−7.33 (m, 2H). ^{13}C NMR (101 MHz, DMSO-d_6) δ 155.17, 153.36, 150.36, 149.45, 134.58, 132.48, 130.97, 130.44, 130.37, 129.22, 129.00, 128.47, 126.41, 114.50, 109.48. HRMS (AP-ESI) m/z, calcd for $C_{21}H_{14}N_6OS_2$, ([M + H]$^+$): 431.0743, found: 431.0739. HPLC t_R = 7.605 min (99.01% purity).

*(Z)-4-(2-(5-Oxo-3-phenyl-4-(2-(thiazol-2-yl)hydrazineylidene)-4,5-dihydro-1H-pyrazol-1-yl)thiazol-4-yl)benzoic Acid (**3**).* The title compound was synthesized from 4-(2-bromoacetyl)benzoic acid, thiosemicarbazide, and intermediate **1** in a manner similar to that described for the preparation of compound **2**, yield: 48%, mp 268−269 °C. ^{1}H NMR (400 MHz, DMSO-d_6) δ 8.16 (d, J = 7.4 Hz, 2H), 8.14−8.11 (m, 2H), 8.06−8.01 (m, 3H), 7.73 (d, J = 4.1 Hz, 1H), 7.60−7.51 (m, 3H), 7.38 (d, J = 4.0 Hz, 1H). ^{13}C NMR (101 MHz, DMSO-d_6) δ 179.37, 167.55, 155.33, 153.46, 149.60, 149.30, 138.42, 132.15, 130.88, 130.47, 130.41, 130.36, 130.33, 128.99, 128.50, 126.37, 114.52, 111.81. HRMS (AP-ESI) m/z, calcd for $C_{22}H_{14}N_6O_3S_2$, ([M + H]$^+$): 475.0642, found: 475.0634. HPLC t_R = 6.454 min (97.78% purity).

*(Z)-N-Hydroxy-4-(2-(5-oxo-3-phenyl-4-(2-(thiazol-2-yl)-hydrazineylidene)-4,5-dihydro-1H-pyrazol-1-yl)thiazol-4-yl)-benzamide (**4**).* To a solution of compound **3** (1.59 g, 4 mmol) in DMF (30 mL) at 0 °C, isobutyl chloroformate (0.61 mL, 4.8 mmol) and *N*-methylmorpholine (0.58 mL, 5.2 mmol) were added and the mixture was stirred for 30 min. It was filtered, and the filtrate was added to freshly prepared hydroxylamine (0.53 g, 16 mmol) in methanol. After stirring the mixture for another 6 h at room temperature, the reaction mixture was poured into 120 mL of H_2O. Filter and the crude product was purified by silica gel column chromatography to obtain the title compound 0.65 g, yield: 45%, mp 194−195 °C. ^{1}H NMR (400 MHz, DMSO-d_6) δ 11.29 (s, 1H), 9.05 (s, 1H), 8.23−7.93 (m, 5H), 7.86 (d, J = 8.1 Hz, 2H), 7.72 (d, J = 3.9 Hz, 1H), 7.55 (q, J = 7.2 Hz, 3H), 7.35 (d, J = 3.9 Hz, 1H). ^{13}C NMR (101 MHz, DMSO-d_6) δ 179.76, 164.39, 155.40, 149.41, 137.04, 133.69, 132.33, 131.20, 130.35, 130.26, 129.25, 128.91, 128.51, 127.90, 126.23, 114.76, 110.95. HRMS (AP-ESI) m/z, calcd for $C_{22}H_{15}N_7O_3S_2$, ([M + H]$^+$): 490.0751, found: 490.0746. HPLC t_R = 16.209 min (98.64% purity).

*Methyl 5-(4-Acetylbenzamido)pentanoate (**5**).* To a solution of 4-carboxybenzaldehyde (1.64 g, 10 mmol), DIPEA (1.65 mL, 10 mmol) and HATU (4.56 g, 12 mmol) were added, and the mixture was stirred for 30 min at room temperature. After adding methyl 5-aminopentanoate hydrochloride (2.01 g, 11 mmol), the mixture was stirred at room temperature overnight. The reaction solution was washed with 1 M HCl, saturated $NaHCO_3$, and saturated brine. The organic phase was dried and concentrated in vacuo to give the crude product. The crude product was purified by silica gel column chromatography to obtain a white solid 2.35 g, yield: 85%, mp 89−90 °C. ^{1}H NMR (400 MHz, $CDCl_3$) δ 8.01 (d, J = 8.1 Hz, 2H), 7.87 (d, J = 8.0 Hz, 2H), 6.48 (s, 1H), 3.69 (s, 3H), 3.49 (q, J = 6.2 Hz, 2H), 2.64 (s, 3H), 2.40 (t, J = 6.7 Hz, 2H), 1.72 (qd, J = 14.1, 7.0 Hz, 4H).

*Methyl 6-(4-Acetylbenzamido)hexanoate (**6**).* The title compound was synthesized from 4-carboxybenzaldehyde and methyl 6-aminohexanoate hydrochloride in a manner similar to that described for the preparation of compound **5**, yield: 67%, mp 96−98°C. ^{1}H NMR (400 MHz, $CDCl_3$) δ 8.00 (d, J = 7.9 Hz, 2H), 7.86 (d, J = 7.9 Hz, 2H), 6.38 (s, 1H), 3.67 (s, 3H), 3.49 (q, J = 6.6 Hz, 2H), 2.64 (s, 3H), 2.34 (t, J = 7.3 Hz, 2H), 1.76−1.60 (m, 4H), 1.50−1.34 (m, 2H).

*Methyl 7-(4-Acetylbenzamido)heptanoate (**7**).* The title compound was synthesized from 4-carboxybenzaldehyde and methyl 7-aminoheptanoate hydrochloride in a manner similar to that described for the preparation of compound **5**, yield: 96%, mp 101−103 °C. ^{1}H NMR (400 MHz, DMSO-d_6) δ 8.62 (t, J = 5.1 Hz, 1H), 8.02 (d, J = 7.6 Hz, 2H), 7.94 (d, J = 8.0 Hz, 2H), 3.57 (s, 3H), 3.26 (dd, J = 12.9, 6.5 Hz, 2H), 2.62 (s, 3H), 2.30 (t, J = 7.3 Hz, 2H), 1.53 (s, 4H), 1.30 (s, 4H).

*Methyl 4-((4-Acetylbenzamido)methyl)benzoate (**8**).* The title compound was synthesized from 4-carboxybenzaldehyde and methyl 4-(aminomethyl)benzoate hydrochloride in a manner similar to that described for the preparation of compound **5**, yield: 99%, mp 132−134°C. ^{1}H NMR (600 MHz, $CDCl_3$) δ 8.03−7.99 (m, 4H), 7.90 (d, J = 8.4 Hz, 2H), 7.42 (d, J = 8.4 Hz, 2H), 6.78 (t, J = 6.0 Hz, 1H), 4.72 (d, J = 5.9 Hz, 2H), 3.91 (s, 3H), 2.63 (s, 3H).

*Methyl (E)-3-(4-((4-Acetylbenzamido)methyl)phenyl)acrylate (**9**).* The title compound was synthesized from 4-carboxybenzaldehyde and methyl (*E*)-3-(4-(aminomethyl)phenyl)acrylate hydrochloride in a manner similar to that described for the preparation of compound **5**, yield: 71%, mp 175−176°C. ^{1}H NMR (400 MHz, DMSO-d_6) δ 9.28 (t, J = 5.7 Hz, 1H), 8.04 (q, J = 8.1 Hz, 4H), 7.70 (d, J = 7.8 Hz, 2H), 7.66 (d, J = 16.0 Hz, 1H), 7.38 (d, J = 7.8 Hz, 2H), 6.63 (d, J = 16.0 Hz, 1H), 4.53 (d, J = 5.8 Hz, 2H), 3.73 (s, 3H), 2.63 (s, 3H).

https://dx.doi.org/10.1021/acs.jmedchem.0c01454
J. Med. Chem. XXXX, XXX, XXX−XXX

*Methyl 5-(4-(2-Bromoacetyl)benzamido)pentanoate (**10**).* To a solution of methyl 5-(4-acetylbenzamido)pentanoate (2.3 g, 8.3 mmol) in chloroform (40 mL) and ethyl acetate (40 mL), copper(II) bromide (3.71 g, 16.6 mmol) was added. Then, the reaction mixture was refluxed for 3 h. It was filtered, and the filtrate was concentrated under reduced pressure. The residues were dissolved with ethyl acetate and washed with water. They were dried over, and the solvent was removed. The crude product was purified by silica gel column chromatography to obtain a white solid 2.24 g, yield: 72%, mp 82−84 °C. ^{1}H NMR (400 MHz, $CDCl_3$) δ 8.05 (d, J = 8.1 Hz, 2H), 7.90 (d, J = 8.1 Hz, 2H), 6.48 (s, 1H), 4.46 (s, 2H), 3.69 (s, 3H), 3.49 (q, J = 6.2 Hz, 2H), 2.40 (t, J = 6.7 Hz, 2H), 1.80−1.65 (m, 4H).

*Methyl 6-(4-(2-Bromoacetyl)benzamido)hexanoate (**11**).* The title compound was synthesized from intermediate **6** in a manner similar to that described for the preparation of compound **10**, yield: 70%, mp 97−99 °C. ^{1}H NMR (400 MHz, DMSO-d_6) δ 8.66 (s, 1H), 8.07 (d, J = 8.0 Hz, 2H), 7.96 (d, J = 7.7 Hz, 2H), 4.98 (s, 2H), 3.57 (s, 3H), 3.26 (dd, J = 12.4, 6.2 Hz, 2H), 2.31 (t, J = 7.3 Hz, 2H), 1.64−1.43 (m, 4H), 1.38−1.26 (m, 2H).

*Methyl 7-(4-(2-Bromoacetyl)benzamido)heptanoate (**12**).* The title compound was synthesized from intermediate **7** in a manner similar to that described for the preparation of compound **10**, yield: 80%, mp 99−101 °C. ^{1}H NMR (400 MHz, $CDCl_3$) δ 8.04 (d, J = 7.9 Hz, 2H), 7.87 (d, J = 7.9 Hz, 2H), 6.23 (s, 1H), 4.46 (s, 2H), 3.67 (s, 3H), 3.47 (dd, J = 13.3, 6.6 Hz, 2H), 2.32 (t, J = 7.4 Hz, 2H), 1.64 (dd, J = 14.1, 7.1 Hz, 4H), 1.50−1.33 (m, 4H).

*Methyl 4-((4-(2-Bromoacetyl)benzamido)methyl)benzoate (**13**).* The title compound was synthesized from intermediate **8** in a manner similar to that described for the preparation of compound **10**, yield: 76%, mp 126−129 °C. ^{1}H NMR (400 MHz, DMSO-d_6) δ 9.36 (dd, J = 13.5, 6.7 Hz, 1H), 8.14−8.01 (m, 4H), 7.94 (d, J = 7.7 Hz, 2H), 7.47 (d, J = 7.9 Hz, 2H), 5.00 (s, 2H), 4.58 (d, J = 5.7 Hz, 2H), 3.84 (s, 3H).

*Methyl (E)-3-(4-((4-(2-Bromoacetyl)benzamido)methyl)phenyl)acrylate (**14**).* The title compound was synthesized from intermediate **9** in a manner similar to that described for the preparation of compound **10**, yield: 63%, mp 149−151 °C. ^{1}H NMR (400 MHz, $CDCl_3$) δ 8.05 (d, J = 8.1 Hz, 2H), 7.91 (d, J = 8.0 Hz, 2H), 7.68 (d, J = 16.0 Hz, 1H), 7.52 (d, J = 7.8 Hz, 2H), 7.38 (d, J = 7.9 Hz, 2H), 6.54 (s, 1H), 6.43 (d, J = 16.0 Hz, 1H), 4.69 (d, J = 5.7 Hz, 2H), 4.45 (s, 2H), 3.81 (s, 3H).

*Methyl (Z)-5-(4-(2-(5-Oxo-3-phenyl-4-(2-(thiazol-2-yl)hydrazineylidene)-4,5-dihydro-1H-pyrazol-1-yl)thiazol-4-yl)benzamido)pentanoate (**15**).* To the solution of methyl 5-(4-(2-bromoacetyl)benzamido)pentanoate (0.42 g, 1 mmol) in methanol (20 mL), thiosemicarbazide (0.09 g, 1 mmol) was added, and the mixture was stirred for 1 h at room temperature. When the addition of the solution of ethyl (*Z*)-3-oxo-3-phenyl-2-(2-(thiazol-2-yl)hydrazono)propanoate (0.36 g, 1 mmol) in methanol (10 mL) was completed, it was refluxed for another 3 h. The reaction mixture was cooled down, and the product was isolated by filtration. It was washed with cold methanol and diethyl ether, and compound **15** was obtained as a red solid 0.28 g, yield: 64%, mp 196−197 °C. ^{1}H NMR (400 MHz, DMSO-d_6) δ 8.53 (t, J = 5.4 Hz, 1H), 8.16 (d, J = 6.7 Hz, 2H), 8.08 (d, J = 7.9 Hz, 2H), 7.98 (s, 1H), 7.93 (d, J = 8.1 Hz, 2H), 7.73 (d, J = 4.0 Hz, 1H), 7.60−7.51 (m, 3H), 7.37 (d, J = 3.9 Hz, 1H), 3.59 (s, 3H), 3.28 (d, J = 5.6 Hz, 2H), 2.36 (t, J = 6.7 Hz, 2H), 1.66−1.48 (m, 4H).

*Methyl (Z)-6-(4-(2-(5-Oxo-3-phenyl-4-(2-(thiazol-2-yl)hydrazineylidene)-4,5-dihydro-1H-pyrazol-1-yl)thiazol-4-yl)benzamido)hexanoate (**16**).* The title compound was synthesized with intermediate **11**, ethyl (*Z*)-3-oxo-3-phenyl-2-(2-(thiazol-2-yl)hydrazono)propanoate, and thiosemicarbazide in a manner similar to that described for the preparation of compound **15**, yield: 59%, mp 199−200 °C. ^{1}H NMR (400 MHz, DMSO-d_6) δ 8.52 (s, 1H), 8.16 (s, 2H), 8.07 (s, 2H), 8.01−7.84 (m, 3H), 7.73 (s, 1H), 7.55 (s, 3H), 7.37 (s, 1H), 3.58 (s, 3H), 3.26 (s, 2H), 2.37−2.24 (m, 2H), 1.61−1.45 (m, 4H), 1.39−1.29 (m, 2H).

*Methyl (Z)-7-(4-(2-(5-Oxo-3-phenyl-4-(2-(thiazol-2-yl)hydrazineylidene)-4,5-dihydro-1H-pyrazol-1-yl)thiazol-4-yl)benzamido)heptanoate (**17**).* The title compound was synthesized from intermediate **12**, ethyl (*Z*)-3-oxo-3-phenyl-2-(2-(thiazol-2-yl)hydrazono)propanoate, and thiosemicarbazide in a manner similar to that described for the preparation of compound **15**, yield: 60%, mp 219−220 °C. ^{1}H NMR (400 MHz, DMSO-d_6) δ 8.50 (t, J = 5.2 Hz, 1H), 8.17 (d, J = 6.8 Hz, 2H), 8.07 (d, J = 7.8 Hz, 2H), 7.98 (s, 1H), 7.93 (d, J = 7.8 Hz, 2H), 7.73 (d, J = 3.7 Hz, 1H), 7.63−7.49 (m, 3H), 7.37 (d, J = 3.9 Hz, 1H), 3.58 (s, 3H), 3.27 (q, J = 6.1 Hz, 2H), 2.31 (t, J = 7.3 Hz, 2H), 1.54 (m, 4H), 1.32 (m, 4H).

*Methyl (Z)-4-((4-(2-(5-Oxo-3-phenyl-4-(2-(thiazol-2-yl)hydrazineylidene)-4,5-dihydro-1H-pyrazol-1-yl)thiazol-4-yl)benzamido)methyl)benzoate (**18**).* The title compound was synthesized from intermediate **13**, ethyl (*Z*)-3-oxo-3-phenyl-2-(2-(thiazol-2-yl)hydrazono)propanoate, and thiosemicarbazide in a manner similar to that described for the preparation of compound **15**, yield: 33%, mp 182−183 °C. ^{1}H NMR (600 MHz, DMSO-d_6) δ 9.20 (t, J = 6.0 Hz, 1H), 8.17 (d, J = 7.4 Hz, 2H), 8.12 (dd, J = 9.5, 7.6 Hz, 2H), 8.04 (d, J = 6.5 Hz, 1H), 8.01 (d, J = 9.1 Hz, 2H), 7.97−7.93 (m, 2H), 7.73 (d, J = 4.1 Hz, 1H), 7.60−7.53 (m, 4H), 7.51−7.47 (m, 2H), 7.37 (d, J = 4.0 Hz, 1H), 4.59 (d, J = 5.9 Hz, 2H), 3.85 (s, 3H).

*Methyl (E)-3-(4-((4-(2-((Z)-5-Oxo-3-phenyl-4-(2-(thiazol-2-yl)hydrazineylidene)-4,5-dihydro-1H-pyrazol-1-yl)thiazol-4-yl)benzamido)methyl)phenyl)acrylate (**19**).* The title compound was synthesized with intermediate **14**, ethyl (*Z*)-3-oxo-3-phenyl-2-(2-(thiazol-2-yl)hydrazono)propanoate, and thiosemicarbazide in a manner similar to that described for the preparation of compound **15**, yield: 68%, mp 250−251 °C. ^{1}H NMR (400 MHz, DMSO-d_6) δ 9.16 (t, J = 5.6 Hz, 1H), 8.16 (d, J = 6.7 Hz, 2H), 8.11 (d, J = 7.8 Hz, 2H), 8.00 (d, J = 7.0 Hz, 3H), 7.74 (d, J = 3.8 Hz, 1H), 7.70 (d, J = 7.6 Hz, 2H), 7.66 (d, J = 16.3 Hz, 1H), 7.56 (d, J = 6.5 Hz, 2H), 7.38 (t, J = 6.0 Hz, 3H), 6.62 (d, J = 16.0 Hz, 1H), 4.53 (d, J = 5.4 Hz, 2H), 3.72 (s, 3H).

*(Z)-N-(5-(Hydroxyamino)-5-oxopentyl)-4-(2-(5-oxo-3-phenyl-4-(2-(thiazol-2-yl)hydrazineylidene)-4,5-dihydro-1H-pyrazol-1-yl)-thiazol-4-yl)benzamide (**20**).* Hydroxylamine hydrochloride (2.92 g, 42 mmol) and potassium hydroxide (3.53 g, 63 mmol) were dissolved in 21 and 15 mL of methyl alcohol, respectively. The solution of potassium hydroxide was added into the solution of hydroxylamine hydrochloride at 0 °C. After 10 min, the reaction mixture was filtered. To the solution of compound **15** (1.76 g, 3 mmol) in DMF (8 mL), freshly prepared hydroxylamine solution was added. The reaction mixture was stirred for 3 h, and the solvent was removed in vacuo. Then, 10 mL of water was added, and the solution was acidified to pH = 4 and then filtered. The crude product was purified by silica gel column chromatography as a red solid 0.97 g, yield: 55%, mp 219−220 °C. ^{1}H NMR (400 MHz, DMSO-d_6) δ 10.37 (s, 1H), 8.54 (t, J = 5.2 Hz, 1H), 8.17 (d, J = 6.9 Hz, 2H), 8.08 (d, J = 7.9 Hz, 2H), 7.98 (s, 1H), 7.94 (d, J = 7.8 Hz, 2H), 7.73 (d, J = 3.7 Hz, 1H), 7.61−7.50 (m, 3H), 7.37 (d, J = 3.6 Hz, 1H), 3.27 (t, J = 5.1 Hz, 2H), 1.99 (t, J = 6.2 Hz, 2H), 1.62−1.45 (m, 4H). ^{13}C NMR (101 MHz, DMSO-d_6) δ 179.49, 174.94, 169.56, 166.22, 155.34, 153.47, 149.51, 136.87, 134.23, 133.06, 131.03, 130.34, 129.76, 128.93, 128.51, 128.15, 126.10, 114.64, 110.95, 39.48, 32.54, 29.31, 23.29. HRMS (AP-ESI) m/z, calcd for $C_{27}H_{24}N_8O_4S_2$, ([M + H]$^+$): 589.1435, found: 589.1422. HPLC t_R = 8.293 min (98.95% purity).

*(Z)-N-(6-(Hydroxyamino)-6-oxohexyl)-4-(2-(5-oxo-3-phenyl-4-(2-(thiazol-2-yl)hydrazineylidene)-4,5-dihydro-1H-pyrazol-1-yl)-thiazol-4-yl)benzamide (**21**).* The title compound was synthesized with intermediate **16** in a manner similar to that described for the preparation of compound **20**, yield: 46%, mp >280 °C. ^{1}H NMR (400 MHz, DMSO-d_6) δ 10.37 (s, 1H), 8.67 (s, 1H), 8.54 (s, 1H), 8.19 (d, J = 6.3 Hz, 2H), 8.07 (d, J = 8.0 Hz, 2H), 7.93 (d, J = 7.9 Hz, 2H), 7.89 (s, 1H), 7.68 (d, J = 2.7 Hz, 1H), 7.50 (dd, J = 14.1, 7.2 Hz, 3H), 7.30 (d, J = 3.5 Hz, 1H), 3.26 (d, J = 6.4 Hz, 2H), 1.96 (t, J = 7.1 Hz, 2H), 1.53 (s, 4H), 1.30 (d, J = 6.5 Hz, 2H). ^{13}C NMR (101 MHz, DMSO-d_6) δ 182.94, 169.59, 166.24, 155.91, 153.45, 150.30, 149.03, 141.82, 137.26, 134.00, 133.22, 129.14, 128.59, 128.14, 126.03, 122.52, 116.12, 110.20, 49.07, 32.72, 29.42, 26.63, 25.43. HRMS (AP-ESI) m/z, calcd for $C_{28}H_{26}N_8O_4S_2$, ([M + H]$^+$): 603.1591, found: 603.1589. HPLC t_R = 13.034 min (97.31% purity).

https://dx.doi.org/10.1021/acs.jmedchem.0c01454
J. Med. Chem. XXXX, XXX, XXX−XXX

*(Z)-N-(7-(Hydroxyamino)-7-oxoheptyl)-4-(2-(5-oxo-3-phenyl-4-(2-(thiazol-2-yl)hydrazineylidene)-4,5-dihydro-1H-pyrazol-1-yl)-thiazol-4-yl)benzamide (**22**).* The title compound was synthesized with intermediate **17** in a manner similar to that described for the preparation of compound **20**, yield: 77%, mp 187−188 °C. ^{1}H NMR (400 MHz, DMSO-d_6) δ 10.35 (s, 1H), 8.51 (t, J = 5.2 Hz, 1H), 8.17 (d, J = 6.8 Hz, 2H), 8.07 (d, J = 7.8 Hz, 2H), 7.98 (s, 1H), 7.93 (d, J = 7.9 Hz, 2H), 7.73 (d, J = 3.7 Hz, 1H), 7.62−7.50 (m, 3H), 7.37 (d, J = 3.7 Hz, 1H), 3.27 (d, J = 6.2 Hz, 2H), 1.95 (t, J = 7.2 Hz, 2H), 1.63−1.44 (m, 4H), 1.38−1.22 (m, 4H). ^{13}C NMR (101 MHz, DMSO-d_6) δ 179.77, 169.61, 166.18, 155.35, 153.40, 149.65, 149.53, 136.83, 134.31, 132.81, 131.07, 130.37, 129.92, 128.96, 128.52, 128.17, 126.09, 114.61, 110.96, 39.70, 32.73, 29.55, 28.85, 26.75, 25.59. HRMS (AP-ESI) m/z, calcd for $C_{29}H_{28}N_8O_4S_2$, ([M + H]$^+$): 617.1748, found: 617.1735. HPLC t_R = 11.52 min (97.88% purity).

*(Z)-N-Hydroxy-4-((4-(2-(5-oxo-3-phenyl-4-(2-(thiazol-2-yl)-hydrazineylidene)-4,5-dihydro-1H-pyrazol-1-yl)thiazol-4-yl)-benzamido)methyl)benzamide (**23**).* The title compound was synthesized with intermediate **18** in a manner similar to that described for the preparation of compound **20**, yield: 29%, mp 217−219 °C. ^{1}H NMR (400 MHz, DMSO-d_6) δ 12.86 (s, 1H), 11.18 (s, 1H), 9.15 (s, 1H), 8.99 (s, 1H), 8.19 (d, J = 6.3 Hz, 1H), 8.11 (d, J = 7.9 Hz, 1H), 8.05−7.84 (m, 6H), 7.72 (d, J = 7.7 Hz, 2H), 7.66 (d, J = 2.9 Hz, 1H), 7.56−7.37 (m, 4H), 7.26 (d, J = 3.1 Hz, 1H), 4.54 (s, 2H). ^{13}C NMR (101 MHz, DMSO-d_6) δ 179.58, 166.45, 164.64, 155.43, 153.53, 149.67, 149.44, 143.48, 137.21, 133.89, 133.73, 131.79, 131.20, 130.25, 129.15, 128.90, 128.53, 128.31, 127.63, 127.46, 126.21, 114.79, 111.07, 42.99. HRMS (AP-ESI) m/z, calcd for $C_{30}H_{22}N_8O_4S_2$, ([M + H]$^+$): 623.1278, found: 623.1270. HPLC t_R = 14.884 min (97.12% purity).

*N-(4-((E)-3-(Hydroxyamino)-3-oxoprop-1-en-1-yl)benzyl)-4-(2-((Z)-5-oxo-3-phenyl-4-(2-(thiazol-2-yl)hydrazineylidene)-4,5-dihydro-1H-pyrazol-1-yl)thiazol-4-yl)benzamide (**24**).* The title compound was synthesized with intermediate **19** in a manner similar to that described for the preparation of compound **20**, yield: 36%, mp 251−253°C. ^{1}H NMR (400 MHz, DMSO-d_6) δ 12.34 (s, 1H), 10.09 (s, 1H), 9.15 (t, J = 5.9 Hz, 1H), 8.18 (d, J = 6.7 Hz, 2H), 8.10 (d, J = 7.8 Hz, 2H), 8.00 (d, J = 7.9 Hz, 2H), 7.94 (s, 1H), 7.77−7.64 (m, 3H), 7.60 (d, J = 15.9 Hz, 1H), 7.53 (m, 3H), 7.38 (d, J = 7.7 Hz, 2H), 7.32 (d, J = 3.3 Hz, 1H), 6.50 (d, J = 15.9 Hz, 1H), 4.53 (d, J = 5.6 Hz, 2H). ^{13}C NMR (101 MHz, DMSO-d_6) δ 181.07, 168.08, 166.42, 155.60, 153.45, 149.26, 144.21, 142.59, 137.31, 133.70, 133.29, 131.97, 129.87, 128.90, 128.81, 128.73, 128.58, 128.29, 128.21, 127.94, 127.20, 126.17, 119.20, 115.14, 110.80, 42.99. HRMS (AP-ESI) m/z, calcd for $C_{32}H_{24}N_8O_4S_2$, ([M + H]$^+$): 649.1435, found: 649.1445. HPLC t_R = 9.004 min (98.36% purity).

*Methyl 4-(4-Acetylphenoxy)butanoate (**25**).* A solution of 4′-hydroxyacetophenone (2.7 g, 20 mmol) in DMF was mixed with K_2CO_3 (8.3 g, 60 mmol); then, methyl 4-bromobutanoate (3.77 mL, 30 mmol) and KI (0.1 g) were added to the solution. The mixture was stirred at room temperature overnight, and the mixture was poured into cool water. It was extracted with ethyl acetate three times, and the organic phases were combined. It was dried over with anhydrous magnesium sulfate for 0.5 h, and then it was filtered. The solvent was removed, and the crude product was purified using silica gel column chromatography to obtain a white solid 3.94 g, yield: 83%, mp 64−66 °C. ^{1}H NMR (400 MHz, $CDCl_3$) δ 7.92 (d, J = 8.2 Hz, 2H), 6.91 (d, J = 8.3 Hz, 2H), 4.08 (t, J = 6.0 Hz, 2H), 3.70 (s, 3H), 2.55 (s, 3H), 2.53 (d, J = 7.4 Hz, 2H), 2.14 (p, J = 6.6 Hz, 2H).

*Methyl 5-(4-Acetylphenoxy)pentanoate (**26**).* The title compound was synthesized with 4′-hydroxyacetophenone and methyl 5-bromopentanoate in a manner similar to that described for the preparation of compound **25**, yield: 90%, mp 56−57 °C. ^{1}H NMR (400 MHz, $CDCl_3$) δ 7.92 (d, J = 8.2 Hz, 2H), 6.91 (d, J = 8.2 Hz, 2H), 4.03 (d, J = 5.2 Hz, 2H), 3.68 (s, 3H), 2.55 (s, 3H), 2.41 (t, J = 6.2 Hz, 2H), 1.92−1.76 (m, 4H).

*Methyl 6-(4-Acetylphenoxy)hexanoate (**27**).* The title compound was synthesized with 4′-hydroxyacetophenone and methyl 6-bromohexanoate in a manner similar to that described for the preparation of compound **25**, yield: 94%, mp 46−48 °C. ^{1}H NMR (400 MHz, $CDCl_3$) δ 7.92 (d, J = 8.4 Hz, 2H), 6.91 (d, J = 8.4 Hz, 2H), 4.02 (t, J = 6.3 Hz, 2H), 3.68 (s, 3H), 2.55 (s, 3H), 2.44−2.31 (m, 2H), 1.94−1.79 (m, 2H), 1.72 (dt, J = 15.2, 7.4 Hz, 2H), 1.52 (dt, J = 15.1, 7.7 Hz, 2H).

*Methyl 7-(4-Acetylphenoxy)heptanoate (**28**).* The title compound was synthesized with 4′-hydroxyacetophenone and methyl 7-bromoheptanoate in a manner similar to that described for the preparation of compound **25**, yield: 90%, mp 63−65 °C. ^{1}H NMR (400 MHz, $CDCl_3$) δ 7.92 (d, J = 8.1 Hz, 2H), 6.91 (d, J = 8.2 Hz, 2H), 4.02 (t, J = 6.4 Hz, 2H), 3.67 (s, 3H), 2.55 (s, 3H), 2.33 (t, J = 7.4 Hz, 2H), 1.89−1.76 (m, 2H), 1.74−1.62 (m, 2H), 1.50 (dt, J = 14.8, 7.3 Hz, 2H), 1.40 (dt, J = 14.7, 7.4 Hz, 2H).

*Methyl 8-(4-Acetylphenoxy)octanoate (**29**).* The title compound was synthesized with 4′-hydroxyacetophenone and methyl 8-bromooctanoate in a manner similar to that described for the preparation of compound **25**, yield: 92%, mp 52−54 °C. ^{1}H NMR (400 MHz, $CDCl_3$) δ 7.92 (d, J = 8.4 Hz, 2H), 6.91 (d, J = 8.4 Hz, 2H), 4.01 (t, J = 6.4 Hz, 2H), 3.67 (s, 3H), 2.55 (s, 3H), 2.32 (t, J = 7.4 Hz, 2H), 1.79 (dq, J = 13.4, 6.6 Hz, 2H), 1.64 (dt, J = 12.1, 6.2 Hz, 2H), 1.56−1.44 (m, 2H), 1.43−1.26 (m, 4H).

*Methyl 4-((4-Acetylphenoxy)methyl)benzoate (**30**).* The title compound was synthesized with 4′-hydroxyacetophenone and methyl 4-(bromomethyl)benzoate in a manner similar to that described for the preparation of compound **25**, yield: 88%, mp 119−121 °C. ^{1}H NMR (400 MHz, $CDCl_3$) δ 8.07 (d, J = 7.8 Hz, 2H), 7.94 (d, J = 8.3 Hz, 2H), 7.50 (d, J = 7.9 Hz, 2H), 7.00 (d, J = 8.3 Hz, 2H), 5.19 (s, 2H), 3.93 (s, 3H), 2.56 (s, 3H).

*Methyl (E)-3-(4-((4-Acetylphenoxy)methyl)phenyl)acrylate (**31**).* The title compound was synthesized with 4′-hydroxyacetophenone and methyl (*E*)-3-(4-(bromomethyl)phenyl)acrylate in a manner similar to that described for the preparation of compound **25**, yield: 84%, mp 150−151 °C. ^{1}H NMR (400 MHz, $CDCl_3$) δ 7.94 (d, J = 8.3 Hz, 2H), 7.68 (t, J = 15.4 Hz, 1H), 7.55 (d, J = 7.9 Hz, 2H), 7.45 (d, J = 7.9 Hz, 2H), 7.00 (d, J = 8.4 Hz, 2H), 6.45 (d, J = 16.0 Hz, 1H), 5.15 (s, 2H), 3.81 (s, 3H), 2.55 (s, 3H).

*Methyl 4-(4-(2-Bromoacetyl)phenoxy)butanoate (**32**).* The title compound was synthesized with intermediate **25** and copper(II) bromide in a manner similar to that described for the preparation of compound **10**, yield: 70%, mp 90−92 °C. ^{1}H NMR (400 MHz, $CDCl_3$) δ 7.96 (d, J = 7.9 Hz, 2H), 6.94 (d, J = 8.2 Hz, 2H), 4.40 (s, 2H), 4.10 (dd, J = 12.4, 6.3 Hz, 2H), 3.70 (s, 3H), 2.54 (t, J = 7.1 Hz, 2H), 2.22−2.09 (m, 2H).

*Methyl 5-(4-(2-Bromoacetyl)phenoxy)pentanoate (**33**).* The title compound was synthesized with intermediate **26** and copper(II) bromide in a manner similar to that described for the preparation of compound **10**, yield: 83%, mp 61−62 °C. ^{1}H NMR (400 MHz, $CDCl_3$) δ 7.95 (d, J = 8.6 Hz, 2H), 6.94 (d, J = 8.6 Hz, 2H), 4.40 (s, 2H), 4.05 (d, J = 5.4 Hz, 2H), 3.68 (s, 3H), 2.41 (t, J = 6.3 Hz, 2H), 1.92−1.77 (m, 4H).

*Methyl 6-(4-(2-Bromoacetyl)phenoxy)hexanoate (**34**).* The title compound was synthesized with intermediate **27** and copper(II) bromide in a manner similar to that described for the preparation of compound **10**, yield: 65%, mp 61−63 °C. ^{1}H NMR (400 MHz, $CDCl_3$) δ 7.96 (d, J = 8.3 Hz, 2H), 6.94 (d, J = 8.3 Hz, 2H), 4.40 (s, 2H), 4.04 (t, J = 6.1 Hz, 2H), 3.68 (s, 3H), 2.36 (t, J = 7.4 Hz, 2H), 1.90−1.79 (m, 2H), 1.78−1.67 (m, 2H), 1.57−1.47 (m, 2H).

*Methyl 7-(4-(2-Bromoacetyl)phenoxy)heptanoate (**35**).* The title compound was synthesized with intermediate **28** and copper(II) bromide in a manner similar to that described for the preparation of compound **10**, yield: 57%, mp 60−61 °C. ^{1}H NMR (400 MHz, $CDCl_3$) δ 7.96 (d, J = 8.3 Hz, 2H), 6.94 (d, J = 8.3 Hz, 2H), 4.40 (s, 2H), 4.08−4.00 (m, 2H), 3.67 (s, 3H), 2.33 (t, J = 7.3 Hz, 2H), 1.89−1.77 (m, 2H), 1.68 (dd, J = 14.9, 7.4 Hz, 2H), 1.50 (dt, J = 14.2, 6.9 Hz, 2H), 1.40 (dt, J = 14.6, 7.4 Hz, 2H).

*Methyl 8-(4-(2-Bromoacetyl)phenoxy)octanoate (**36**).* The title compound was synthesized with intermediate **29** and copper(II) bromide in a manner similar to that described for the preparation of compound **10**, yield: 53%, mp 62−64 °C. ^{1}H NMR (400 MHz, $CDCl_3$) δ 7.96 (d, J = 8.6 Hz, 2H), 6.94 (d, J = 8.6 Hz, 2H), 4.40 (s, 2H), 4.03 (t, J = 6.3 Hz, 2H), 3.67 (s, 3H), 2.32 (t, J = 7.4 Hz, 2H),

https://dx.doi.org/10.1021/acs.jmedchem.0c01454
J. Med. Chem. XXXX, XXX, XXX−XXX

1.89−1.75 (m, 2H), 1.64 (dt, J = 14.5, 7.4 Hz, 2H), 1.55−1.44 (m, 2H), 1.44−1.31 (m, 4H).

*Methyl 4-((4-(2-Bromoacetyl)phenoxy)methyl)benzoate (**37**).* The title compound was synthesized with intermediate **30** and copper(II) bromide in a manner similar to that described for the preparation of compound **10**, yield: 84%, mp 121−123 °C. ^{1}H NMR (400 MHz, $CDCl_3$) δ 8.07 (d, J = 7.7 Hz, 2H), 7.98 (d, J = 8.2 Hz, 2H), 7.50 (d, J = 7.9 Hz, 2H), 7.03 (d, J = 8.2 Hz, 2H), 5.21 (s, 2H), 4.39 (s, 2H), 3.93 (s, 3H).

*Methyl (E)-3-(4-((4-(2-Bromoacetyl)phenoxy)methyl)phenyl)acrylate (**38**).* The title compound was synthesized with intermediate **31** and copper(II) bromide in a manner similar to that described for the preparation of compound **10**, yield: 75%, mp 140−141 °C. ^{1}H NMR (400 MHz, $CDCl_3$) δ 7.97 (d, J = 8.4 Hz, 2H), 7.70 (d, J = 16.0 Hz, 1H), 7.56 (d, J = 7.8 Hz, 2H), 7.45 (d, J = 7.8 Hz, 2H), 7.03 (d, J = 8.4 Hz, 2H), 6.46 (d, J = 16.0 Hz, 1H), 5.16 (s, 2H), 4.39 (s, 2H), 3.81 (s, 3H).

*Methyl (Z)-4-(4-(2-(5-Oxo-3-phenyl-4-(2-(thiazol-2-yl)hydrazineylidene)-4,5-dihydro-1H-pyrazol-1-yl)thiazol-4-yl)phenoxy)butanoate (**39**).* The title compound was synthesized from intermediate **32**, ethyl (*Z*)-3-oxo-3-phenyl-2-(2-(thiazol-2-yl)hydrazono)propanoate, and thiosemicarbazide in a manner similar to that described for the preparation of compound **15**, yield: 52%, mp 196−198 °C. ^{1}H NMR (400 MHz, DMSO-d_6) δ 8.16 (d, J = 7.0 Hz, 2H), 7.91 (d, J = 8.0 Hz, 2H), 7.72 (d, J = 3.7 Hz, 1H), 7.66 (s, 1H), 7.61−7.51 (m, 3H), 7.36 (d, J = 3.7 Hz, 1H), 7.01 (d, J = 8.1 Hz, 2H), 4.04 (t, J = 6.1 Hz, 2H), 3.62 (s, 3H), 2.50−2.46 (m, 2H), 2.10−1.94 (m, 2H).

*Methyl (Z)-5-(4-(2-(5-Oxo-3-phenyl-4-(2-(thiazol-2-yl)hydrazineylidene)-4,5-dihydro-1H-pyrazol-1-yl)thiazol-4-yl)phenoxy)pentanoate (**40**).* The title compound was synthesized from intermediate **33**, ethyl (*Z*)-3-oxo-3-phenyl-2-(2-(thiazol-2-yl)hydrazono)propanoate, and thiosemicarbazide in a manner similar to that described for the preparation of compound **15**, yield: 54%, mp 173−174 °C. ^{1}H NMR (400 MHz, DMSO-d_6) δ 8.16 (d, J = 6.9 Hz, 2H), 7.91 (d, J = 8.1 Hz, 2H), 7.72 (d, J = 3.8 Hz, 1H), 7.66 (s, 1H), 7.63−7.48 (m, 3H), 7.37 (d, J = 3.8 Hz, 1H), 7.01 (d, J = 8.1 Hz, 2H), 4.13−3.94 (m, 2H), 3.60 (s, 3H), 2.40 (t, J = 6.8 Hz, 2H), 1.73 (dd, J = 12.3, 6.5 Hz, 4H).

*Methyl (Z)-6-(4-(2-(5-Oxo-3-phenyl-4-(2-(thiazol-2-yl)hydrazineylidene)-4,5-dihydro-1H-pyrazol-1-yl)thiazol-4-yl)phenoxy)hexanoate (**41**).* The title compound was synthesized from intermediate **34**, ethyl (*Z*)-3-oxo-3-phenyl-2-(2-(thiazol-2-yl)hydrazono)propanoate, and thiosemicarbazide in a manner similar to that described for the preparation of compound **15**, yield: 71%, mp 198−200 °C. ^{1}H NMR (400 MHz, DMSO-d_6) δ 8.16 (d, J = 6.9 Hz, 2H), 7.91 (d, J = 8.1 Hz, 2H), 7.72 (d, J = 3.7 Hz, 1H), 7.66 (s, 1H), 7.63−7.50 (m, 3H), 7.36 (d, J = 3.7 Hz, 1H), 7.00 (d, J = 8.1 Hz, 2H), 4.00 (t, J = 6.2 Hz, 2H), 3.59 (s, 3H), 2.34 (t, J = 7.3 Hz, 2H), 1.73 (dd, J = 13.7, 6.6 Hz, 2H), 1.61 (dt, J = 14.7, 7.2 Hz, 2H), 1.54−1.38 (m, 2H).

*Methyl (Z)-7-(4-(2-(5-Oxo-3-phenyl-4-(2-(thiazol-2-yl)hydrazineylidene)-4,5-dihydro-1H-pyrazol-1-yl)thiazol-4-yl)phenoxy)heptanoate (**42**).* The title compound was synthesized from intermediate **35**, ethyl (*Z*)-3-oxo-3-phenyl-2-(2-(thiazol-2-yl)hydrazono)propanoate, and thiosemicarbazide in a manner similar to that described for the preparation of compound **15**, yield: 68%, mp 146−147 °C. ^{1}H NMR (400 MHz, DMSO-d_6) δ 8.16 (d, J = 7.0 Hz, 2H), 7.90 (d, J = 8.0 Hz, 2H), 7.72 (d, J = 3.7 Hz, 1H), 7.66 (s, 1H), 7.54 (t, J = 9.9 Hz, 3H), 7.36 (d, J = 3.8 Hz, 1H), 7.00 (d, J = 8.2 Hz, 2H), 4.00 (t, J = 6.2 Hz, 2H), 3.59 (s, 3H), 2.32 (t, J = 7.3 Hz, 2H), 1.72 (dd, J = 13.6, 6.7 Hz, 2H), 1.63−1.51 (m, 2H), 1.48−1.39 (m, 2H), 1.39−1.30 (m, 2H).

*Methyl (Z)-8-(4-(2-(5-Oxo-3-phenyl-4-(2-(thiazol-2-yl)hydrazineylidene)-4,5-dihydro-1H-pyrazol-1-yl)thiazol-4-yl)phenoxy)octanoate (**43**).* The title compound was synthesized from intermediate **36**, ethyl (*Z*)-3-oxo-3-phenyl-2-(2-(thiazol-2-yl)hydrazono)propanoate, and thiosemicarbazide in a manner similar to that described for the preparation of compound **15**, yield: 76%, mp 166−167 °C. ^{1}H NMR (400 MHz, DMSO-d_6) δ 8.16 (d, J = 6.8 Hz, 2H), 7.90 (d, J = 8.1 Hz, 2H), 7.72 (d, J = 3.4 Hz, 1H), 7.66 (s, 1H), 7.63−7.49 (m, 3H), 7.37 (d, J = 3.7 Hz, 1H), 7.00 (d, J = 8.0 Hz, 2H), 4.01 (t, J = 6.2 Hz, 2H), 3.58 (s, 3H), 2.30 (t, J = 7.6 Hz, 2H), 1.72 (dd, J = 13.4, 6.6 Hz, 2H), 1.60−1.50 (m, 2H), 1.42 (d, J = 6.7 Hz, 2H), 1.32 (m, 4H).

*Methyl (Z)-4-((4-(2-(5-Oxo-3-phenyl-4-(2-(thiazol-2-yl)hydrazineylidene)-4,5-dihydro-1H-pyrazol-1-yl)thiazol-4-yl)phenoxy)methyl)benzoate (**44**).* The title compound was synthesized from intermediate **37**, ethyl (*Z*)-3-oxo-3-phenyl-2-(2-(thiazol-2-yl)hydrazono)propanoate, and thiosemicarbazide in a manner similar to that described for the preparation of compound **15**, yield: 61%, mp 215−216 °C. ^{1}H NMR (400 MHz, DMSO-d_6) δ 8.16 (d, J = 6.9 Hz, 2H), 8.00 (d, J = 7.5 Hz, 2H), 7.94 (d, J = 8.1 Hz, 2H), 7.72 (d, J = 3.7 Hz, 1H), 7.69 (s, 1H), 7.63 (d, J = 8.1 Hz, 2H), 7.60−7.50 (m, 3H), 7.37 (d, J = 3.7 Hz, 1H), 7.12 (d, J = 8.2 Hz, 2H), 5.27 (s, 2H), 3.86 (s, 3H).

*Methyl (E)-3-(4-((4-(2-((Z)-5-Oxo-3-phenyl-4-(2-(thiazol-2-yl)hydrazineylidene)-4,5-dihydro-1H-pyrazol-1-yl)thiazol-4-yl)phenoxy)methyl)phenyl)acrylate (**45**).* The title compound was synthesized from intermediate **38**, ethyl (*Z*)-3-oxo-3-phenyl-2-(2-(thiazol-2-yl)hydrazono)propanoate, and thiosemicarbazide in a manner similar to that described for the preparation of compound **15**, yield: 78%, mp 222−223 °C. ^{1}H NMR (400 MHz, DMSO-d_6) δ 8.16 (d, J = 6.8 Hz, 2H), 7.93 (d, J = 8.2 Hz, 2H), 7.76 (d, J = 7.8 Hz, 2H), 7.72 (d, J = 4.0 Hz, 1H), 7.71−7.64 (m, 2H), 7.53 (m, 5H), 7.37 (d, J = 3.7 Hz, 1H), 7.11 (d, J = 8.3 Hz, 2H), 6.66 (d, J = 16.0 Hz, 1H), 5.21 (s, 2H), 3.73 (s, 3H).

*(Z)-N-Hydroxy-4-(4-(2-(5-oxo-3-phenyl-4-(2-(thiazol-2-yl)hydrazineylidene)-4,5-dihydro-1H-pyrazol-1-yl)thiazol-4-yl)phenoxy)butanamide (**46**).* The title compound was synthesized with intermediate **39** in a manner similar to that described for the preparation of compound **20**, yield: 67%, mp 242−244 °C. ^{1}H NMR (400 MHz, DMSO-d_6) δ 10.44 (s, 1H), 8.72 (s, 1H), 8.21 (d, J = 6.5 Hz, 2H), 7.91 (d, J = 8.1 Hz, 2H), 7.64 (s, 1H), 7.57−7.38 (m, 4H), 7.25 (d, J = 2.7 Hz, 1H), 7.00 (d, J = 8.2 Hz, 2H), 4.01 (t, J = 6.1 Hz, 2H), 2.16 (t, J = 7.2 Hz, 2H), 2.02−1.90 (m, 2H). ^{13}C NMR (101 MHz, DMSO) δ 182.87, 169.13, 158.71, 155.61, 153.40, 149.95, 149.71, 141.20, 133.19, 129.11, 128.85, 128.58, 127.88, 127.70, 123.08, 115.82, 115.00, 106.49, 67.32, 29.24, 25.34. HRMS (AP-ESI) m/z, calcd for $C_{25}H_{21}N_7O_4S_2$, ([M + H]$^+$): 548.1169, found: 548.1170. HPLC t_R = 13.493 min (99.75% purity).

*(Z)-N-Hydroxy-5-(4-(2-(5-oxo-3-phenyl-4-(2-(thiazol-2-yl)hydrazineylidene)-4,5-dihydro-1H-pyrazol-1-yl)thiazol-4-yl)phenoxy)pentanamide (**47**).* The title compound was synthesized with intermediate **40** in a manner similar to that described for the preparation of compound **20**, yield: 83%, mp 153−155 °C. ^{1}H NMR (400 MHz, DMSO-d_6) δ 10.39 (s, 1H), 8.69 (s, 1H), 8.19 (d, J = 6.6 Hz, 2H), 7.91 (d, J = 8.3 Hz, 2H), 7.67 (d, J = 3.2 Hz, 1H), 7.57 (s, 1H), 7.49 (dt, J = 21.4, 7.3 Hz, 3H), 7.29 (d, J = 3.2 Hz, 1H), 7.01 (d, J = 8.3 Hz, 2H), 4.01 (d, J = 5.8 Hz, 2H), 2.04 (t, J = 6.6 Hz, 2H), 1.80−1.61 (m, 4H). ^{13}C NMR (101 MHz, DMSO-d_6) δ 181.73, 169.44, 158.86, 155.43, 153.42, 149.97, 149.74, 138.27, 132.38, 129.60, 128.75, 128.51, 127.72, 127.61, 125.59, 115.48, 115.00, 106.82, 67.56, 32.40, 28.68, 22.28. HRMS (AP-ESI) m/z, calcd for $C_{26}H_{23}N_7O_4S_2$, ([M + H]$^+$): 562.1326, found: 562.1320. HPLC t_R = 6.208 min (96.77% purity).

*(Z)-N-Hydroxy-6-(4-(2-(5-oxo-3-phenyl-4-(2-(thiazol-2-yl)hydrazineylidene)-4,5-dihydro-1H-pyrazol-1-yl)thiazol-4-yl)phenoxy)hexanamide (**48**).* The title compound was synthesized with intermediate **41** in a manner similar to that described for the preparation of compound **20**, yield: 55%, mp 132−134 °C. ^{1}H NMR (400 MHz, DMSO-d_6) δ 10.35 (s, 1H), 8.16 (d, J = 6.9 Hz, 1H), 7.91 (d, J = 8.2 Hz, 1H), 7.72 (d, J = 3.5 Hz, 1H), 7.66 (s, 1H), 7.60−7.49 (m, 1H), 7.36 (d, J = 3.7 Hz, 1H), 7.01 (d, J = 8.2 Hz, 1H), 4.00 (t, J = 6.0 Hz, 1H), 1.99 (t, J = 7.1 Hz, 1H), 1.78−1.69 (m, 1H), 1.56 (dd, J = 14.4, 7.1 Hz, 1H), 1.48−1.37 (m, 1H). ^{13}C NMR (101 MHz, DMSO-d_6) δ 179.00, 172.51, 169.52, 159.01, 154.98, 153.43, 150.29, 149.32, 132.75, 130.92, 130.42, 130.31, 128.99, 128.44, 127.75, 127.29, 114.99, 114.52, 107.31, 67.86, 32.72, 28.94, 25.67, 21.53. HRMS (AP-ESI) m/z, calcd for $C_{27}H_{25}N_7O_4S_2$, ([M + H]$^+$): 576.1482, found: 576.1481. HPLC t_R = 6.721 min (99.98% purity).

https://dx.doi.org/10.1021/acs.jmedchem.0c01454
J. Med. Chem. XXXX, XXX, XXX−XXX

*(Z)-N-Hydroxy-7-(4-(2-(5-oxo-3-phenyl-4-(2-(thiazol-2-yl)-hydrazineylidene)-4,5-dihydro-1H-pyrazol-1-yl)thiazol-4-yl)-phenoxy)heptanamide (**49**).* The title compound was synthesized with intermediate **42** in a manner similar to that described for the preparation of compound **20**, yield: 64%, mp 127−128 °C. ^{1}H NMR (400 MHz, DMSO-d_6) δ 10.33 (s, 1H), 8.16 (d, J = 6.9 Hz, 2H), 7.91 (d, J = 8.0 Hz, 2H), 7.72 (d, J = 3.5 Hz, 1H), 7.65 (s, 1H), 7.61−7.49 (m, 3H), 7.36 (d, J = 3.5 Hz, 1H), 7.01 (d, J = 8.1 Hz, 2H), 4.01 (t, J = 6.2 Hz, 2H), 1.96 (t, J = 7.2 Hz, 2H), 1.78−1.68 (m, 2H), 1.52 (dd, J = 14.6, 7.2 Hz, 2H), 1.47−1.39 (m, 2H), 1.36−1.28 (m, 2H). ^{13}C NMR (101 MHz, DMSO-d_6) δ 179.45, 169.57, 159.03, 155.01, 153.40, 150.28, 149.37, 132.71, 131.00, 130.40, 130.21, 129.00, 128.46, 127.76, 127.30, 115.02, 114.53, 107.30, 67.91, 32.69, 29.09, 28.84, 25.75, 25.56. HRMS (AP-ESI) m/z, calcd for $C_{28}H_{27}N_7O_4S_2$, ([M + H]$^+$): 590.1639, found: 590.1628. HPLC t_R = 12.577 min (97.32% purity).

*(Z)-N-Hydroxy-8-(4-(2-(5-oxo-3-phenyl-4-(2-(thiazol-2-yl)-hydrazineylidene)-4,5-dihydro-1H-pyrazol-1-yl)thiazol-4-yl)-phenoxy)octanamide (**50**).* The title compound was synthesized with intermediate **43** in a manner similar to that described for the preparation of compound **20**, yield: 60%, mp 144−145 °C. ^{1}H NMR (400 MHz, DMSO-d_6) δ 10.32 (s, 1H), 8.16 (d, J = 7.1 Hz, 2H), 7.91 (d, J = 8.2 Hz, 2H), 7.72 (d, J = 3.6 Hz, 1H), 7.65 (s, 1H), 7.61−7.49 (m, 3H), 7.36 (d, J = 3.7 Hz, 1H), 7.01 (d, J = 8.1 Hz, 2H), 4.01 (t, J = 6.2 Hz, 2H), 1.95 (t, J = 7.2 Hz, 2H), 1.80−1.67 (m, 2H), 1.57−1.47 (m, 2H), 1.45−1.38 (m, 2H), 1.37−1.21 (m, 4H). ^{13}C NMR (101 MHz, DMSO-d_6) δ 179.08, 169.62, 159.02, 154.98, 153.42, 150.29, 149.32, 132.76, 130.94, 130.40, 130.27, 128.98, 128.44, 127.75, 127.26, 114.98, 114.53, 107.28, 67.93, 32.73, 29.16, 29.01, 29.00, 25.92, 25.56. HRMS (AP-ESI) m/z, calcd for $C_{29}H_{29}N_7O_4S_2$, ([M + H]$^+$): 604.1795, found: 604.1787. HPLC t_R = 5.994 min (99.01% purity).

*(Z)-N-Hydroxy-4-((4-(2-(5-oxo-3-phenyl-4-(2-(thiazol-2-yl)-hydrazineylidene)-4,5-dihydro-1H-pyrazol-1-yl)thiazol-4-yl)-phenoxy)methyl)benzamide (**51**).* The title compound was synthesized with intermediate **44** in a manner similar to that described for the preparation of compound **20**, yield: 60%, mp 216−217 °C. ^{1}H NMR (400 MHz, DMSO-d_6) δ 11.22 (s, 1H), 9.03 (s, 1H), 8.18 (d, J = 7.0 Hz, 2H), 7.93 (d, J = 8.1 Hz, 2H), 7.78 (d, J = 7.6 Hz, 2H), 7.69 (d, J = 3.3 Hz, 1H), 7.62 (s, 1H), 7.59−7.46 (m, 5H), 7.31 (d, J = 3.2 Hz, 1H), 7.11 (d, J = 8.1 Hz, 2H), 5.22 (s, 2H). ^{13}C NMR (101 MHz, DMSO-d_6) δ 180.80, 172.51, 164.43, 158.43, 155.27, 153.40, 149.94, 140.67, 135.92, 132.73, 131.87, 129.99, 129.96, 129.90, 128.83, 128.51, 127.93, 127.77, 127.52, 115.44, 115.00, 107.22, 69.18. HRMS (AP-ESI) m/z, calcd for $C_{29}H_{21}N_7O_4S_2$, ([M + H]$^+$): 596.1169, found: 596.1156. HPLC t_R = 15.510 min (99.59% purity).

*(E)-N-Hydroxy-3-(4-((4-(2-((Z)-5-oxo-3-phenyl-4-(2-(thiazol-2-yl)-hydrazineylidene)-4,5-dihydro-1H-pyrazol-1-yl)thiazol-4-yl)-phenoxy)methyl)phenyl)acrylamide (**52**).* The title compound was synthesized with intermediate **45** in a manner similar to that described for the preparation of compound **20**, yield: 70%, mp 186−188 °C. ^{1}H NMR (400 MHz, DMSO-d_6) δ 10.77 (s, 1H), 9.13 (s, 1H), 8.16 (d, J = 6.9 Hz, 2H), 7.93 (d, J = 8.2 Hz, 2H), 7.71 (d, J = 3.6 Hz, 1H), 7.66 (s, 1H), 7.53 (ddd, J = 31.3, 21.8, 11.8 Hz, 8H), 7.35 (d, J = 3.6 Hz, 1H), 7.11 (d, J = 8.2 Hz, 2H), 6.48 (d, J = 15.8 Hz, 1H), 5.19 (s, 2H). ^{13}C NMR (101 MHz, DMSO-d_6) δ 179.19, 163.15, 158.56, 155.07, 153.46, 150.17, 149.38, 138.83, 138.42, 134.86, 133.34, 131.07, 130.32, 129.79, 128.95, 128.64, 128.46, 128.07, 127.79, 127.75, 119.66, 115.42, 114.63, 107.48, 69.35. HRMS (AP-ESI) m/z, calcd for $C_{31}H_{23}N_7O_4S_2$, ([M + H]$^+$): 622.1326, found: 622.1320. HPLC t_R = 5.343 min (97.91% purity).

■ ASSOCIATED CONTENT

Supporting Information

The Supporting Information is available free of charge at https://pubs.acs.org/doi/10.1021/acs.jmedchem.0c01454.

Production of recombinant Bax proteins; synthesis of stapled peptides; ^{1}H NMR, ^{13}C NMR, and HRMS spectra of all target compounds; HPLC chromatogram of final products; flow cytometry analysis in HeLa cells and HeLa cells Bax$^{-/-}$; cellular transfections; docking results of compound **23** with Bax; and molecular dynamics simulation of BTSA1 with Bax (PDF)

Molecular formula strings (CSV)

Docking results of BTSA1 with Bax (PDB)

Docking results of compound **23** with Bax (PDB)

■ AUTHOR INFORMATION

Corresponding Author

Hao Fang − *Department of Medicinal Chemistry, Key Laboratory of Chemical Biology (Ministry of Education), School of Pharmaceutical Sciences, Cheeloo College of Medicine, Shandong University, Jinan, Shandong 250012, P. R. China;* orcid.org/0000-0002-2879-5146; Phone: 86-531-88382019; Email: haofangcn@ sdu.edu.cn

Authors

Tao Liang − *Department of Medicinal Chemistry, Key Laboratory of Chemical Biology (Ministry of Education), School of Pharmaceutical Sciences, Cheeloo College of Medicine, Shandong University, Jinan, Shandong 250012, P. R. China*

Yi Zhou − *Department of Medicinal Chemistry, Key Laboratory of Chemical Biology (Ministry of Education), School of Pharmaceutical Sciences, Cheeloo College of Medicine, Shandong University, Jinan, Shandong 250012, P. R. China;* orcid.org/0000-0002-1282-2461

Reham M. Elhassan − *Department of Medicinal Chemistry, Key Laboratory of Chemical Biology (Ministry of Education), School of Pharmaceutical Sciences, Cheeloo College of Medicine, Shandong University, Jinan, Shandong 250012, P. R. China*

Xuben Hou − *Department of Medicinal Chemistry, Key Laboratory of Chemical Biology (Ministry of Education), School of Pharmaceutical Sciences, Cheeloo College of Medicine, Shandong University, Jinan, Shandong 250012, P. R. China;* orcid.org/0000-0002-8346-9001

Xinying Yang − *Department of Medicinal Chemistry, Key Laboratory of Chemical Biology (Ministry of Education), School of Pharmaceutical Sciences, Cheeloo College of Medicine, Shandong University, Jinan, Shandong 250012, P. R. China*

Complete contact information is available at: https://pubs.acs.org/10.1021/acs.jmedchem.0c01454

Notes

The authors declare no competing financial interest.

■ ACKNOWLEDGMENTS

The authors genuinely thank the Advanced Medical Research Institute, Shandong University, for their help in the experiments. They thank Renxiao Wang from Shanghai institute of Organic Chemistry, Chinese Academy of Sciences, for his donation of *E. coli* produced recombinant *N*-terminal His-tagged human Bcl-2, Mcl-1, and Bcl-X_L proteins. This work was supported by the National Nature Science Foundation of China (21672127 and 81874288), the Major Project of Science and Technology of Shandong Province (2017CXGC1401), the Shandong Provincial Natural Science Foundation (ZR2019LZL004), the Fundamental Research Funds of Shandong University (2019GN045), and the Joint Research Funds for Shandong University and Karolinska Institute (SDU-KI-2019-06).

ABBREVIATIONS

HDAC, histone deacetylase; MOM, mitochondrial outer membrane; MOMP, mitochondrial outer membrane permeabilization; BAM7, Bax activator; BTSA1, Bax activator; AML, acute myeloid leukemia; SAHA, Vorinostat, HDAC inhibitor; CTCL, cutaneous T-cell lymphoma; PTCL, peripheral T-cell lymphoma; MM, multiple myeloma; CI, combination index; AIDS, acquired immunodeficiency syndrome; DDI, drug−drug interaction; PK, pharmacokinetics; PD, pharmacodynamic; ZBG, zinc binding group; SAR, structure−activity relationship; THF, tetrahydrofuran; HATU, 1-[bis(dimethylamino)-methylene]-1*H*-1,2,3-triazolo[4,5-*b*]pyridinium 3-oxid hexafluorophosphate; DIPEA, *N*,*N*-diisopropylethylamine; DMF, *N*,*N*-dimethylformamide; FPA, fluorescence polarization assay; FITC-BIM, fluorescein isothiocyanate-labeled stapled peptide of the BIM BH3 helix; IC_{50}, half-maximal inhibitory concentration; TUNEL, terminal deoxynucleotidyl transferase (TdT) dUTP nick-end labeling; PI, propidium iodide; TMRE, tetramethylrhodamine ethyl ester; SEC, size exclusion chromatography; Ac-BIM, acetylated stapled peptide of the BIM BH3 helix; His-Bax, histidine-labeled Bax protein; EC_{50}, concentration for 50% of maximal effect; 5-FAM Bid-BH3, 5-carboxyfluorescein-labeled Bid-BH3 helix; His-Bcl-2, histidine-labeled Bcl-2 protein; His-Bcl-X_L, histidine-labeled Bcl-X_L protein; ABT-199, Bcl-2 inhibitor; AMC, 7-amino-4-methylcoumarin; TSA, trichostatin A, HDAC inhibitor; DMSO, dimethyl sulfoxide; PMSF, phenylmethanesulfonyl fluoride, protease inhibitors; SDS, sodium dodecylsulfate; PAGE, polyacrylamide gel electrophoresis; PVDF, poly(vinylidene fluoride); GAPDH, glyceraldehyde-3-phosphate dehydrogenase; FBS, fetal bovine serum; MTT, 3-(4,5-dimethyl-2-thiazolyl)-2,5-diphenyl-2-*H*-tetrazolium bromide; HL-7702, human normal liver cells; PBS, phosphate-buffered saline; DTT, dithiothreitol; DEVE-AFC, caspase-3 substrates; TLC, thin-layer chromatography

REFERENCES

(1) Forouzanfar, M. H.; Foreman, K. J.; Delossantos, A. M.; Lozano, R.; Lopez, A. D.; Murray, C. J. L.; Naghavi, M. Breast and cervical cancer in 187 countries between 1980 and 2010: a systematic analysis. *Lancet* **2011**, *378*, 1461−1484.

(2) Movva, S.; Rodriguez, L.; Arias-Pulido, H.; Verschraegen, C. Novel chemotherapy approaches for cervical cancer. *Cancer* **2009**, *115*, 3166−3180.

(3) Brave, M.; Dagher, R.; Farrell, A.; Abraham, S.; Ramchandani, R.; Gobburu, J.; Booth, B.; Jiang, X.; Sridhara, R.; Justice, R.; Pazdur, R. Topotecan in combination with cisplatin for the treatment of stage IVB, recurrent, or persistent cervical cancer. *Oncology* **2006**, *20*, 1401−1404.

(4) Al-Mansour, Z.; Verschraegen, C. Locally advanced cervical cancer: What is the standard of care? *Curr. Opin. Oncol.* **2010**, *22*, 503−512.

(5) Rose, P. G.; Eifel, P. J. Combined radiation therapy and chemotherapy for carcinoma of the cervix. *Cancer J.* **2001**, *7*, 86−94.

(6) Roszik, J.; Ring, K. L.; Wani, K. M.; Lazar, A. J.; Yemelyanova, A. V.; Soliman, P. T.; Frumovitz, M.; Jazaeri, A. A. Gene expression analysis identifies novel targets for cervical cancer therapy. *Front. Immunol.* **2018**, *9*, No. 2102.

(7) Won, M.; Luo, Y.; Lee, D. H.; Shin, E.; Suh, D. S.; Kim, T. H.; Jin, H.; Bae, J. BAX is an essential key mediator of AP5M1-induced apoptosis in cervical carcinoma cells. *Biochem. Biophys. Res. Commun.* **2019**, *518*, 368−373.

(8) Cosentino, K.; Garcia-Saez, A. J. Bax and Bak Pores: Are we closing the circle? *Trends Cell Biol.* **2017**, *27*, 266−275.

(9) Kuwana, T.; Mackey, R. M.; Perkins, G.; Ellisman, M. H.; Latterich, M.; Schneiter, R.; Green, D. R.; Newmeyer, D. D. Bid, Bax, and Lipids cooperate to form supramolecular openings in the outer mitochondrial membrane. *Cell* **2002**, *111*, 331−342.

(10) Eskes, R.; Desagher, S.; Antonsson, B.; Martinou, J. C. Bid induces the oligomerization and insertion of Bax into the outer mitochondrial membrane. *Mol. Cell Biol.* **2000**, *20*, 929−935.

(11) Dewson, G.; Kluck, R. M. Mechanisms by which Bak and Bax permeabilise mitochondria during apoptosis. *J. Cell Sci.* **2009**, *122*, 2801−2808.

(12) Czabotar, P. E.; Westphal, D.; Dewson, G.; Ma, S.; Hockings, C.; Fairlie, W. D.; Lee, E. F.; Yao, S.; Robin, A. Y.; Smith, B. J.; Huang, D. C.; Kluck, R. M.; Adams, J. M.; Colman, P. M. Bax crystal structures reveal how BH3 domains activate Bax and nucleate its oligomerization to induce apoptosis. *Cell* **2013**, *152*, 519−531.

(13) Yamaguchi, H.; Bhalla, K.; Wang, H. Bax plays a pivotal role in thapsigargin-induced apoptosis of human colon cancer HCT116 cells by controlling Smac Diablo and Omi HtrA2 release from mitochondria. *Cancer Res.* **2003**, *63*, 1483−1489.

(14) Davids, M. S.; Letai, A. Targeting the B-cell lymphoma/leukemia 2 family in cancer. *J. Clin. Oncol.* **2012**, *30*, 3127−3135.

(15) Davids, M. S.; Letai, A. ABT-199: Taking dead aim at BCL-2. *Cancer Cell* **2013**, *23*, 139−141.

(16) Gavathiotis, E.; Reyna, D. E.; Davis, M. L.; Bird, G. H.; Walensky, L. D. BH3-triggered structural reorganization drives the activation of proapoptotic BAX. *Mol. Cell* **2010**, *40*, 481−492.

(17) Ren, D.; Tu, H.-C.; Kim, H.; Wang, G. X.; Bean, G. R.; Takeuchi, O.; Jeffers, J. R.; Zambetti, G. P.; Hsieh, J. J.-D.; Cheng, E. H.-Y. BID, BIM, and PUMA are essential for activation of the BAX- and BAK-dependent cell death program. *Science* **2010**, *330*, 1390−1393.

(18) Gavathiotis, E.; Reyna, D. E.; Bellairs, J. A.; Leshchiner, E. S.; Walensky, L. D. Direct and selective small-molecule activation of proapoptotic BAX. *Nat. Chem. Biol.* **2012**, *8*, 639−645.

(19) Reyna, D. E.; Garner, T. P.; Lopez, A.; Kopp, F.; Choudhary, G. S.; Sridharan, A.; Narayanagari, S. R.; Mitchell, K.; Dong, B.; Bartholdy, B. A.; Walensky, L. D.; Verma, A.; Steidl, U.; Gavathiotis, E. Direct activation of BAX by BTSA1 overcomes apoptosis resistance in acute myeloid leukemia. *Cancer Cell* **2017**, *32*, 490−505.

(20) Stornaiuolo, M.; La Regina, G.; Passacantilli, S.; Grassia, G.; Coluccia, A.; La Pietra, V.; Giustiniano, M.; Cassese, H.; Di Maro, S.; Brancaccio, D.; Taliani, S.; Ialenti, A.; Silvestri, R.; Martini, C.; Novellino, E.; Marinelli, L. Structure-based lead optimization and biological evaluation of BAX direct activators as novel potential anticancer agents. *J. Med. Chem.* **2015**, *58*, 2135−2148.

(21) Pritz, J. R.; Wachter, F.; Lee, S.; Luccarelli, J.; Wales, T. E.; Cohen, D. T.; Coote, P.; Heffron, G. J.; Engen, J. R.; Massefski, W.; Walensky, L. D. Allosteric sensitization of proapoptotic BAX. *Nat. Chem. Biol.* **2017**, *13*, 961−967.

(22) Duvic, M.; Vu, J. Vorinostat: a new oral histone deacetylase inhibitor approved for cutaneous T-cell lymphoma. *Expert Opin. Invest. Drugs* **2007**, *16*, 1111−1120.

(23) Whittaker, S. J.; Demierre, M. F.; Kim, E. J.; Rook, A. H.; Lerner, A.; Duvic, M.; Scarisbrick, J.; Reddy, S.; Robak, T.; Becker, J. C.; Samtsov, A.; McCulloch, W.; Kim, Y. H. Final results from a multicenter, international, pivotal study of romidepsin in refractory cutaneous T-cell lymphoma. *J. Clin. Oncol.* **2010**, *28*, 4485−4491.

(24) Poole, R. M. Belinostat: first global approval. *Drugs* **2014**, *74*, 1543−1554.

(25) Garnockjones, K. P. Panobinostat: First global approval. *Drugs* **2015**, *75*, 695−704.

(26) Ning, Z.; Li, Z.; Newman, M. J.; Shan, S.; Wang, X.; Pan, D.; Zhang, J.; Dong, M.; Du, X.; Lu, X. Chidamide (CS055/HBI-8000): a new histone deacetylase inhibitor of the benzamide class with antitumor activity and the ability to enhance immune cell-mediated tumor cell cytotoxicity. *Cancer Chemother. Pharmacol.* **2012**, *69*, 901−909.

https://dx.doi.org/10.1021/acs.jmedchem.0c01454
J. Med. Chem. XXXX, XXX, XXX−XXX

(27) Zhao, B.; He, T. Chidamide, a histone deacetylase inhibitor, functions as a tumor inhibitor by modulating the ratio of Bax/Bcl-2 and P21 in pancreatic cancer. *Oncol. Rep.* **2015**, *33*, 304−310.
(28) Maiso, P.; Colado, E.; Ocio, E. M.; Garayoa, M.; Martin, J.; Atadja, P.; Pandiella, A.; San-Miguel, J. F. The synergy of panobinostat plus doxorubicin in acute myeloid leukemia suggests a role for HDAC inhibitors in the control of DNA repair. *Leukemia* **2009**, *23*, 2265−2274.
(29) Wang, J.; Kim, T. H.; Ahn, M. Y.; Lee, J.; Jung, J. H.; Choi, W. S.; Lee, B. M.; Yoon, K. S.; Yoon, S.; Kim, H. S. Sirtinol, a class III HDAC inhibitor, induces apoptotic and autophagic cell death in MCF-7 human breast cancer cells. *Int. J. Oncol.* **2012**, *41*, 1101−1109.
(30) Chou, T. C. Drug combination studies and their synergy quantification using the Chou-Talalay method. *Cancer Res.* **2010**, *70*, 440−446.
(31) Yuan, S.; Wang, F.; Chen, G.; Zhang, H.; Feng, L.; Wang, L.; Colman, H.; Keating, M. J.; Li, X.; Xu, R. H.; Wang, J.; Huang, P. Effective elimination of cancer stem cells by a novel drug combination strategy. *Stem Cells* **2013**, *31*, 23−34.
(32) Zahedi, P.; Souza, R. D.; Huynh, L.; Piquette-Miller, M.; Allen, C. Combination drug delivery strategy for the treatment of multidrug resistant ovarian cancer. *Mol Pharmaceutics* **2011**, *8*, 260−269.
(33) Madani Tonekaboni, S. A.; Soltan Ghoraie, L.; Manem, V. S. K.; Haibe-Kains, B. Predictive approaches for drug combination discovery in cancer. *Briefings Bioinf.* **2018**, *19*, 263−276.
(34) Luna-Vargas, M. P. A.; Chipuk, J. E. Physiological and pharmacological control of BAK, BAX, and beyond. *Trends Cell Biol.* **2016**, *26*, 906−917.
(35) Morphy, R.; Kay, C.; Rankovic, Z. From magic bullets to designed multiple ligands. *Drug Discovery Today* **2004**, *9*, 641−651.
(36) de Lera, A. R.; Ganesan, A. Epigenetic polypharmacology: from combination therapy to multitargeted drugs. *Clin. Epigenet.* **2016**, *8*, No. 105.
(37) Anighoro, A.; Bajorath, J.; Rastelli, G. Polypharmacology: challenges and opportunities in drug discovery. *J. Med. Chem.* **2014**, *57*, 7874−7887.
(38) Yang, E. G.; Mustafa, N.; Tan, E. C.; Poulsen, A.; Ramanujulu, P. M.; Chng, W. J.; Yen, J. J.; Dymock, B. W. Design and Synthesis of Janus Kinase 2 (JAK2) and Histone Deacetlyase (HDAC) Bispecific Inhibitors Based on Pacritinib and Evidence of Dual Pathway Inhibition in Hematological Cell Lines. *J. Med. Chem.* **2016**, *59*, 8233−8262.
(39) Zhou, Y.; Liu, X.; Xue, J.; Liu, L.; Liang, T.; Li, W.; Yang, X.; Hou, X.; Fang, H. Discovery of peptide boronate derivatives as histone deacetylase and proteasome dual inhibitors for overcoming bortezomib resistance of multiple myeloma. *J. Med. Chem.* **2020**, *63*, 4701−4715.
(40) Bertrand, P. Inside HDAC with HDAC inhibitors. *Eur J. Med. Chem.* **2010**, *45*, 2095−2116.

https://dx.doi.org/10.1021/acs.jmedchem.0c01454
J. Med. Chem. XXXX, XXX, XXX−XXX